

Quantized Response and Topology of Insulators with Inversion Symmetry

Ari M. Turner, Yi Zhang, Roger S. K. Mong, Ashvin Vishwanath
Department of Physics, University of California, Berkeley, California 94720, USA
 (Dated: December 30, 2018)

We study three dimensional insulators with inversion symmetry, in which other point group symmetries, such as time reversal, are generically absent. Their band topology is found to be classified by the parities of occupied states at time reversal invariant momenta (TRIM parities), and by three Chern numbers. The TRIM parities of any insulator must satisfy a constraint: their product must be $+1$. The TRIM parities also constrain the Chern numbers modulo two. When the Chern numbers vanish, a magneto-electric response parameterized by θ is defined and is quantized to $\theta = 0, \pi$. Its value is entirely determined by the TRIM parities. These results may be useful in the search for magnetic topological insulators with large θ . A classification of inversion symmetric insulators is also given for general dimensions. An alternate geometrical derivation of our results is obtained by using the entanglement spectrum of the ground state wave-function.

I. INTRODUCTION

Recently, the discovery of a class of insulator with nontrivial band topology protected by time reversal symmetry¹ has led to a range of discoveries on the qualitative properties of solids. Soon after, it was realized that this is part of a broader classification of gapped topological phases with free fermions. If one includes particle hole symmetry, natural for superconducting Hamiltonians, one ends up with ten symmetry classes^{2,3} that include both insulators and gapped superconductors. The symmetry transformations, time reversal and particle hole symmetry, can be consistently generalized to include disorder and inhomogeneities. Topological phases in these classes are always characterized by protected surface states. However, one can also discuss band topology in the presence of the point group symmetry of a crystal. That is, which classes of Hamiltonians can be smoothly connected to one another while preserving the insulating gap and the symmetry? Although these distinctions require considering a perfect crystal, and inevitably fade in the presence of disorder, one often deals with crystals that are sufficiently clean for such distinctions to be useful.

The general classification is a daunting task, given the vast number of symmetry groups of crystals. For example, there are 230 space groups; if one adds transformation under time reversal symmetry to describe magnetic insulators, one has 1,651 different groups. We focus here on a simple case, inversion ($\mathbf{r} \rightarrow -\mathbf{r}$), a symmetry that is commonly realized in magnetic insulators. For example, all Bravais lattices are inversion symmetric. An additional virtue is that inversion symmetry forces the magnetoelectric response to be isotropic and quantized, allowing us to calculate it by qualitative methods. Here, we will classify the topologically distinct inversion symmetric insulators, and determine their protected properties. (Phases of antiferromagnets can also be classified using a similar approach⁴.)

The classes of three dimensional inversion symmetric insulators are found to be parameterized by three Chern numbers and a set of inversion parities. The Chern num-

bers, which are already present in the absence of inversion symmetry, determine the quantized Hall response. While this is an integer in two dimensions, it is given by a reciprocal lattice vector $\tilde{\mathbf{G}}_H$ in a three dimensional crystal. Inversion parities are the only additional parameters that appear from adding the extra symmetry. They are defined at those momenta that are left invariant under $\mathbf{k} \rightarrow -\mathbf{k}$, up to a reciprocal lattice vector. This defines eight points in the 3D Brillouin Zone - the Time Reversal Invariant Momenta (TRIM). States at these momenta can be classified by their parities, eigenvalues under inversion, which are ± 1 . The set of inversion parities of the filled levels at the TRIMs and $\tilde{\mathbf{G}}_H$ completely specifies the topological class of the insulator.

Usually, distinct topological classes can be distinguished by their surface state content. A different approach is to identify a quantized response, such as Hall conductivity, that can distinguish topological classes. For inversion symmetric insulators, in general, no protected surface states arise. This is due to the fact that although inversion is present in the bulk, it is absent at the surface of the system, which separates an inside from an outside. However, quantized physical response functions exist, and are protected by inversion symmetry. These include the magnetoelectric susceptibility θ , which is defined, for example, as the polarization (\mathbf{P}) induced by a magnetic field (\mathbf{B}), in a parallel direction: $\mathbf{P} = \theta \frac{e^2}{2\pi h} \mathbf{B}$. The coefficient θ requires both bulk and surface to be insulating and is defined modulo 2π . Under time reversal, $\theta \rightarrow -\theta$. Apart from the trivial solution $\theta = 0$, the ambiguity in the definition of θ allows also for $\theta = \pi$. The latter was shown to occur in time reversal symmetric topological insulators, when magnetic perturbations restricted to the surface open a surface gap⁵⁻⁷.

Under inversion symmetry, θ transforms in the same way as under time reversal. Once again we expect $\theta = 0, \pi$. The latter case is particularly interesting since the magnetoelectric susceptibility is large and no extra effort will usually be required to gap out surface states, in contrast to topological insulators. Typically, one does not expect surface modes in the inversion symmetric case. The response θ is determined just by the parities of the

states at TRIMs, according to a formula derived below (which is analogous to formulae for the time reversal-symmetric cases^{6,8,9}). Thus it will be possible to determine the magnetoelectric susceptibility without doing any band integrals. This should be useful in the search for large θ insulators in magnetically ordered materials. Moreover, in magnetic insulators a large spin orbit coupling is not a priori required to obtain the phase with $\theta = \pi$, which opens up a wider selection of candidates.

A second set of results are in the form of constraints on the allowed values of TRIM parities and Chern numbers $\tilde{\mathbf{G}}_H$. We first show that in any insulator, a *parity constraint* is present. The product of the TRIM parities of filled states is always +1. While this is a trivial condition when time reversal is also present, and energy levels come in Kramers pairs, it is rather non-trivial for magnetic insulators. For example, the parity assignment in Fig. 1a rules out a band gap. A corollary of this result is that it is impossible to make a direct continuous transition between a $\theta = 0$ and $\theta = \pi$ insulator, if time reversal is broken. One must either evolve through a non-insulating state, or a first order transition. A continuous transition only exists if both time reversal and inversion are present¹⁰. Another constraint fixes whether the three components of $\tilde{\mathbf{G}}_H$, are even or odd in relation to the TRIM parities. The intrinsic polarization \mathbf{P} of the insulator is also determined by the parities.

Finally we consider the entanglement. The entanglement spectrum of topological insulators contains special modes^{11–13}. Section IV relates the number of gapless modes in the entanglement spectrum to the parity invariants. This result is used to rederive some of the electromagnetic properties in a simple fashion.

The present article addresses some questions left open in earlier work in which we participated. Ref. 12 discusses the entanglement spectrum of inversion symmetric insulators, without presenting the exact relation to TRIM parities. The proofs given here also complete the reasoning presented in¹⁴ which studied the electronic structure of a specific material using the expressions for θ in terms of TRIM parities and the parity constraint.

In the next section, we give a brief survey of all of our results and a guide to the sections where their proofs can be found.

II. SUMMARY OF RESULTS

The phases associated with a given symmetry can be classified using some topology. Each state can be classified by integer-valued parameters (or by integers relative some modulus). These cannot change continuously, so they determine phases.

Let us first define some conventions about the crystal lattice. We will for simplicity assume that the lattice is cubic (although there is no symmetry beyond inversion) and has a lattice spacing equal to one unit. All quantities will be written with respect to a coordinate system

xyz that is aligned with the axes of the crystal. The results may be translated to systems with a *general* Bravais lattice, by interpreting the expressions in the right coordinate system. Let \mathbf{R}_i be the primitive vectors of the lattice and let \mathbf{g}^i be the reciprocal vectors, $\mathbf{g}^i \cdot \mathbf{R}_j = 2\pi\delta_j^i$. If a vector is in real space, the coordinates v^x, v^y, v^z refer to $\mathbf{v} = v^x\mathbf{R}_1 + v^y\mathbf{R}_2 + v^z\mathbf{R}_3$. Vectors \mathbf{u} in reciprocal space should be expanded in terms of reciprocal vectors, $\mathbf{u} = \frac{1}{2\pi}(u_x\mathbf{g}^1 + u_y\mathbf{g}^2 + u_z\mathbf{g}^3)$. Electrical polarization is a real space vector; 3D Hall conductivity and momentum are in reciprocal space (and we also use upper and lower indices on the coordinates as a reminder of what basis to use).

To classify bulk insulators, it is useful to look at inversion parities, as in the study of spectra of small molecules. The main difference is that in solids, the occupied states can be labelled by momentum. Let these states be given by $\psi_{i\mathbf{k}}(\mathbf{r}) = u_{i\mathbf{k}}(\mathbf{r})e^{i\mathbf{k}\cdot\mathbf{r}}$. The parity classification is only useful at the “TRIMs,” the momenta given by

$$\boldsymbol{\kappa} = \frac{n_1}{2}\mathbf{g}_1 + \frac{n_2}{2}\mathbf{g}_2 + \frac{n_3}{2}\mathbf{g}_3 \quad (1)$$

where n_1, n_2, n_3 are integers. Such a momentum maps to itself under inversion symmetry modulo the reciprocal lattice, $-\boldsymbol{\kappa} \equiv \boldsymbol{\kappa}$. Hence the wave functions at $\boldsymbol{\kappa}$ must be invariant, and their parities can be defined:

$$\mathcal{I}\psi_{a\boldsymbol{\kappa}}(\mathbf{r}) = \eta_a(\boldsymbol{\kappa})\psi_{a\boldsymbol{\kappa}}(\mathbf{r}) \quad (2)$$

Appendix B explains how to find these parities using a tight-binding model.

We now introduce a key quantity $n_o(\boldsymbol{\kappa})$ at every TRIM $\boldsymbol{\kappa}$. This is defined as the *number of states with odd parities* at that TRIM. Note, these cannot change without a phase transition (at least in a non-interacting system). Besides these 8 integers, the quantum Hall conductance gives three more invariant integers, since it is quantized: $\mathbf{G}_H = \frac{e^2}{2\pi h}\tilde{\mathbf{G}}_H$ where $\frac{\tilde{\mathbf{G}}_H}{2\pi}$ has integer components (according to the conventions defined above).

These 11 integers, together with the total number of occupied bands n , are the only parameters necessary to determine a phase—any two band structures with the same integers can be tuned into one another without a phase transition. This scheme is derived in Sec. III A. Appendix A gives an alternative method that is easier to generalize. These integers cannot be chosen independently of one another; there are some relationships between their parities. These relationships can help predict material properties, since the parities are easy to determine from the band structure.

Total Parity Constraint: All the constraints can be written in terms of the net parities:

$$\eta_{\boldsymbol{\kappa}} = (-1)^{n_o(\boldsymbol{\kappa})} = \prod_a \eta_a(\boldsymbol{\kappa}). \quad (3)$$

For any insulator, one can show:

$$\prod_{\boldsymbol{\kappa}} \eta_{\boldsymbol{\kappa}} = 1. \quad (4)$$

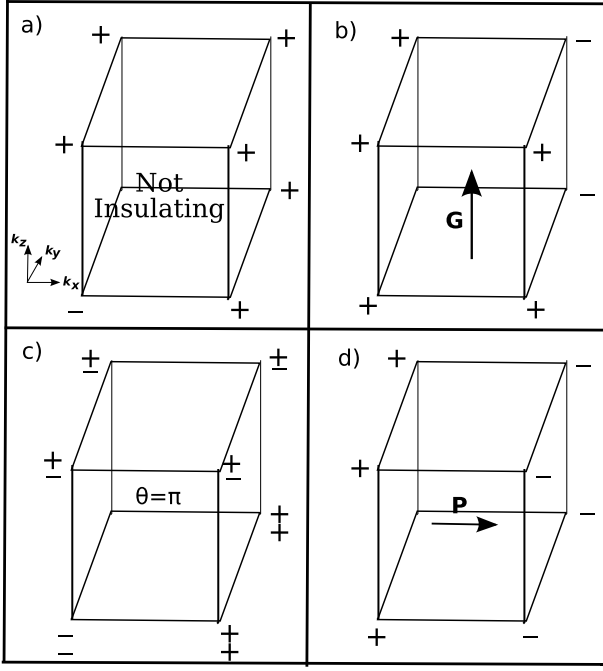


FIG. 1: Determining properties of systems using parities. The boxes represent an eighth of the Brillouin Zone; the TRIMs are at the corners. The signs represent the parities of the occupied states at the TRIMs. In (a) the parity constraint of even number of odd parity states is violated, hence it cannot be an insulator. In (b) the parities require a nonvanishing Hall conductance, with odd Chern number in the $k_x k_y$ planes. (c) Quantized magnetoelectric response $\theta = \pi$ determined from number of odd parity states being $2 \pmod{4}$. (d) A parity configuration corresponding to a frozen polarization.

That is, the total number of filled odd parity states must be even. This is shown in Sec. III B.

If a system has the parities in Fig. 1a, it must be metallic, because the parities do not satisfy Eq. (4). The gap must close at some momentum \mathbf{k} in the Brillouin zone. The simplest case is if the system is a semimetal, with a single pair of cone-points at the Fermi energy.

Quantum Hall Effect. Furthermore, the parities determine the quantum Hall integers modulo 2. The parity of $\frac{\tilde{G}_{H,z}}{2\pi}$ is constrained; e.g. the z -component satisfies

$$e^{\frac{i}{2}\tilde{G}_{H,z}} = \prod_{\substack{\kappa; \\ \kappa \cdot \mathbf{R}_z = 0}} \eta_{\kappa} \quad (5)$$

That is, whether the Hall conductivity along the z -direction is an even or odd multiple of 2π can be determined by multiplying the η 's around either of the squares parallel to the xy -plane. This result is derived in Sec. III C.

If a system has the parities shown in Fig. 1b, the Hall conductivity cannot vanish. The component along the z -direction, $G_{H,z}$, must be an odd multiple of $\frac{e^2}{hc}$ (per layer of the crystal).

Eqs. (4),(5) are the only relationships between the

invariants—if the relationships are satisfied, the invariants can be realized in principle.

Magnetoelectric Effect. The most interesting electromagnetic response that we discuss is the magnetoelectric polarizability α_j^i . An applied magnetic field induces a polarization, $P^i = \alpha_j^i B^j$. In the absence of the quantum Hall effect, α_j^i is well-defined. (Otherwise the polarization can be neutralized by a flow of charge in the surface states associated with the Hall effect.) The polarizability α_j^i is odd under inversion: Under inversion symmetry, \mathbf{P} changes sign, while \mathbf{B} does not.

If the crystal is inversion symmetric, it seems that α must vanish. However, α is ambiguous like the polarization. An isotropic portion ($\frac{e^2}{h}\delta_{ij} \times \text{integer}$) is indeterminate. (The magnetoelectric effect affects only properties of the surface of a crystal. An integer magnetoelectric effect can be mimicked by a quantum Hall coating on the surface.) Thus α_j^i can be isotropic, $\frac{e^2}{2\pi h}\theta\delta_j^i$, if θ is a multiple of π . To determine θ , the η_{κ} parameters are not sufficient, and we must return to the n_o 's:

$$\frac{\theta}{\pi} \equiv \frac{1}{2} \sum_{\kappa} n_o(\kappa) \pmod{2}. \quad (6)$$

According to Eq. (4), this is always an integer. This expression is proved in Sec. III D.

Fig. 1c shows the parities of a model with 2 filled bands, which has a nontrivial θ . The total number of odd states at all the TRIMs is twice an odd number, hence θ is π . One interpretation of $\theta = \pi$ is that the insulator has a half-integer quantum-Hall effect on the surface. Two filled bands are necessary for a nontrivial θ . The requirement $\mathbf{G}_H = 0$ implies, for one filled band, that the number of states is a multiple of 4. (See Eq. (7 in the next section.)

Frozen Polarization. Finally, let us discuss what information is contained in the “net parities” η_{κ} . Eq. (5) shows that they determine the Chern numbers modulo 2. This accounts for three of the eight parities. Note that any pattern of parities satisfying the constraint Eq. (4) can be factored into 7 basis patterns:

$$\eta(\kappa) = \pm(-1)^{\frac{1}{2\pi^3}(\tilde{G}_{H,x}\kappa_y\kappa_z + \tilde{G}_{H,y}\kappa_x\kappa_z + \tilde{G}_{H,z}\kappa_x\kappa_y)} (-1)^{\frac{2}{\pi}\tilde{\mathbf{P}}_e \cdot \kappa}, \quad (7)$$

where the components of $\tilde{\mathbf{P}}_e$ are half-integers and the components of $\tilde{\mathbf{G}}_H$ are integers times 2π . (The factors of π are added to make the exponents into integers.) This equation agrees with Eq. (5), so $\tilde{\mathbf{G}}_H$ is the Hall conductivity modulo 2. When $\tilde{\mathbf{G}}_H = 0$, η_{κ} varies as a plane wave on the vertices of the cube. The components of $\tilde{\mathbf{P}}_e$ determine the intrinsic polarization.

A crystal may have an intrinsic polarization when the Hall conductivity is zero¹⁵; in this case, η_{κ} looks like a plane wave on the vertices of the cube (see Fig. 1d) and $\tilde{\mathbf{P}}_e$ is the wave-number. The spontaneous electrical polarization is similar to θ ; it is defined only¹⁵ modulo a lattice vector times e . Inversion symmetry constrains the components to be integers or half-integers times e .

Hence the polarization is determined by three bits and Eq. (7) gives all the information about the polarization that can be obtained from bulk properties. To get the polarization correct, one needs to include the offset between the electrons and the compensating charges in the nuclei:

$$\mathbf{P} = e\tilde{\mathbf{P}}_e - \sum_i Z_i e \mathbf{r}_{Ni}, \quad (8)$$

where \mathbf{r}_{Ni} is the position vector of the i^{th} nucleus, with charge $-Z_i e$. This result is derived in Sec. III C.

Consider the polarization of the crystal with the band structure illustrated in Fig. 1d; it is $\frac{e}{2}\mathbf{R}_1$ if the nuclei are all on the sites of the Bravais lattice. This intrinsic dipole moment may correspond to actual ferroelectricity; the crystal would have a surface charge and a large electric field. Alternatively, the translational symmetry of the surface may be spontaneously broken or the surface may be metallic (see Ref. 16 which is summarized in appendix F).

Parity constraints in general dimensions. The results in higher dimensions have a surprising feature: as the number of dimensions increases the sum of the n_o 's must be divisible by larger and larger powers of 2.

Specifically, in $2s$ -dimensions, the sum of the n_o 's is a multiple of 2^{s-1} . This multiple is related to the $2s$ -dimensional Chern number \tilde{G}_{2s} (defined as a multiple of 2π):

$$\frac{1}{2^{s-1}} \sum_{\text{TRIM } \kappa} n_o(\kappa) \equiv \frac{s^{\text{th}} \text{ Chern number}}{2\pi} \pmod{2}; \quad (9)$$

the quantum Hall conductance is the 2-dimensional special case.

In $2s+1$ -dimensions, the sum of the n_o 's is a multiple of 2^s and is related to the Chern-Simons integral

$$\frac{\theta_{2s+1}}{\pi} = \frac{1}{2^s} \sum_{\kappa} n_o(\kappa) \pmod{2}. \quad (10)$$

where the polarization and magnetoelectric effect are the one- and three-dimensional versions.

Note that insulators with inversion symmetry are quite different from ones: There is an insulator in $2s$ dimensions with a Chern number \tilde{G}_{2s} equal to 1 which has just s filled bands²⁴ This insulator is not inversion symmetric, though. The simplest inversion symmetric insulator with the identical Chern number has a minimum of 2^s bands, exponentially more bands than are necessary without symmetry.

The Entanglement Spectrum. An insulator with inversion symmetry has a particle-hole symmetry \mathcal{I}_e in its entanglement spectrum $\epsilon_a(\mathbf{k})$ when it is cut on a plane through a center of inversion. This makes it very easy to determine qualitative properties of the Fermi arcs of the entanglement spectrum—it is possible to count (without topological arguments) the number of zero modes in the

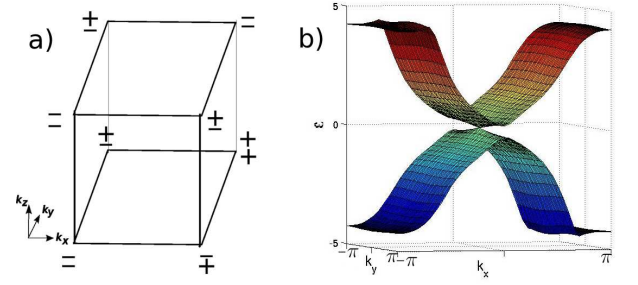


FIG. 2: Entanglement spectrum of a hopping Hamiltonian. a) The parities at the TRIMs. b) The entanglement modes on a cut parallel to the xy -plane. Note that there are two zero-modes at the TRIM $(0,0)$ and none at the other TRIMs, as expected from the parities.

entanglement spectrum at the TRIMs κ_{\perp} along the surface. Let $\Delta N_e(\kappa_{\perp}) = \text{tr}_{\epsilon=0} \mathcal{I}_e$; that is $\Delta N_e(\kappa_{\perp})$ is the number of even modes minus the number of odd modes with zero entanglement-energy at κ_{\perp} .

This can be expressed in terms of parities of the bulk states through $n_o(\kappa)$. Define these parities relative to an inversion center on the plane of the cut. The quantity that appears is $\Delta N(\kappa) = \text{tr}_{E<0} \mathcal{I}$, or $n - 2n_o(\kappa)$:

$$\Delta N_e(\kappa_{\perp}) = \frac{1}{2}(\Delta N(\kappa_1) + \Delta N(\kappa_2)), \quad (11)$$

where κ_1 and κ_2 are the two TRIMs that project to κ_{\perp} . In words: the difference between the number of even and odd states on the entanglement “Fermi surface” at a TRIM is half the difference between the even and odd states in the bulk, at the corresponding TRIMs.

To illustrate an actual entanglement spectrum, we constructed a Hamiltonian with a cubic unit cell whose inversion parities suggest that $\theta = \pi$ and $\tilde{G}_{Hi} \equiv 0 \pmod{2}$. The parities and the spectrum are shown in Fig. 2. (The Hamiltonian is described in Appendix B.) The entanglement spectrum was calculated for a cut along the xy -plane. As expected, there is a Dirac point at $(0,0)$. In this case, there are no chiral modes.

From the relation between the entanglement spectrum and the parities, one can give alternative derivations of some of the results described above. This formula also leads to a simple determination of Fu and Kane’s formula for the indices of topological insulators. These indices describe the number (modulo 2) of physical surface states on a line connecting two TRIMs, and these states are easy to count for the entanglement spectrum. The entanglement spectrum can be continuously deformed into the physical spectrum so it has the same index.

III. ELECTROMAGNETIC EVALUATIONS AND EQUIVALENCE OF INSULATORS

A. Classifying Inversion Symmetric Insulators

This section presents the classification of noninteracting insulators with inversion symmetry. Hamiltonians with inversion symmetry can be related to Hamiltonians without any symmetry, which are already classified by Chern numbers. The only new parameters occurring for inversion symmetry come from the classification of "zero-dimensional insulators", or finite molecules with inversion symmetry.

Consider the Hamiltonian $H(\mathbf{k})$ for the wavefunctions $\psi_{n\mathbf{k}}$. This Hamiltonian can be taken to be an $N \times N$ matrix by using a tight-binding model with N bands (n of which are filled). Since this Hamiltonian is inversion symmetric,

$$I_0 H(\mathbf{k}) I_0 = H(-\mathbf{k}) \quad (12)$$

where I_0 is the matrix describing how the orbitals within the unit cell transform under inversion²⁵.

Assume that H varies continuously without passing through a phase transition. This means that no states ever cross the Fermi energy, $\mu = 0$, say. Let us determine when two Hamiltonians are in the same phase—i.e., can be connected in this way. We wish to find criteria on the matrix fields $H(\mathbf{k})$ that can be used to determine which phase they are in.

The only special points in the Brillouin zones are the TRIMs, κ , which are invariant under inversion symmetry. Each of these points can be interpreted as a zero-dimensional system, with a Hamiltonian $H(\kappa)$ that is invariant under I_0 , since Eq. (12) implies $I_0 H(\kappa) I_0 = H(\kappa)$. Let $n_o(\kappa)$ be the number of eigenvalues at negative energy which are odd under I_0 . The states at this TRIM can mix together, but even states can mix only with even states and odd ones can mix only with odd ones, so the value of $n_o(\kappa)$ cannot change.

The Chern numbers of the Hamiltonian are topological winding numbers which also turn out to describe the Hall conductivity^{17,18}. Because they are integers, they are also invariant.

We will now spend the rest of this section showing that these give a complete classification of Hamiltonians with inversion symmetry. That is, if $H(\mathbf{k})$ and $H'(\mathbf{k})$ are two Hamiltonians with the same number n of occupied states, and the same *total* number of states N , and total number of odd states N_o (both filled and empty bands) and such that

$$\begin{aligned} n_o(\kappa) &= n'_o(\kappa) \text{ (for all TRIMs } \kappa) \\ \tilde{\mathbf{G}}_H &= \tilde{\mathbf{G}}_{H'}, \end{aligned} \quad (13)$$

then (at least if $N - n, n \geq 2$) there is a family of Hamiltonians that connects $H(\mathbf{k})$ to $H'(\mathbf{k})$ without a phase transition and while satisfying Eq. (12). (We may assume that I_0 remains constant since N, N_o do not change.)

We do not usually consider the integers N and N_o to be important invariants—their values can be changed by adding even or odd orbitals with a very high energy. In continuous space, there are infinitely many available orbitals.

The assumption $N - n, n \geq 2$ is included because, when there are too few bands, there are some Hamiltonians that cannot be deformed into one another just because there are not enough degrees of freedom.¹⁹²⁶ Our classification theorem does not capture these distinctions, but the distinctions are not related to any generic properties. If one adds sufficiently many trivial occupied and unoccupied bands to an insulator, any two insulators with the same invariants can be deformed into one another.

Proof for (13): Here we present the essential ideas in the classification of insulators. App. A gives a more systematic way of deriving the classification, including higher dimensions.

This result can be derived by relating a Hamiltonian in d dimensions to one in a smaller number of dimensions. Let us take d to be arbitrary at first, so that we can describe the general reasoning. Let \mathcal{H}_d be the space of general Hamiltonians in d dimensions, while \mathcal{I}_d is the subspace of Hamiltonians that also have inversion symmetry. A generic Hamiltonian in \mathcal{H}_d can be regarded as a closed loop in \mathcal{H}_{d-1} : For each value of k_d (the d^{th} component of \mathbf{k}), consider the $d - 1$ -dimensional Hamiltonian H_{k_d} defined by fixing one component of \mathbf{k} , $H_{k_d}(k_1, k_2, \dots, k_{d-1}) \equiv H(k_1, k_2, \dots, k_d)$. This describes a closed loop because the Brillouin zone is periodic.

A Hamiltonian in \mathcal{I}_d is an arc in \mathcal{H}_{d-1} with end-points in \mathcal{I}_{d-1} (Fig. 3) shows \mathcal{H}_d schematically, with several possible arcs representing Hamiltonians. This arc is constructed by looking at the cross-sections of $H(\mathbf{k})$ between $k_d = 0$ and $k_d = \pi$. The rest of the Hamiltonian can be reconstructed using inversion symmetry. The end-points have to be on \mathcal{I}_{d-1} because the inversion takes the $k_d = 0, \pi$ cross-sections to themselves.

Thus, let us solve the following problem: consider arcs γ_1, γ_2 in \mathcal{H}_{d-1} connecting two points in the subspace \mathcal{I}_{d-1} . What conditions ensure that it is possible to move arc γ_1 to arc γ_2 ? This deformation is possible if we can first slide the end-points of γ_1 within \mathcal{I}_{d-1} onto the end-points of γ_2 and then smoothly deform the curves connecting them. Fig. 3 illustrates the problem.

We can thus classify d -dimensional Hamiltonians by solving two problems: describing the different components of \mathcal{I}_{d-1} , and classifying the arcs connecting a pair of points in \mathcal{H}_{d-1} up to homotopy.

Let us now consider $d = 3$. The first step is analogous to the problem we are trying to solve, just in one dimension less. (The components of \mathcal{I}_2 are just the different classes of 2-dimensional inversion-symmetric Hamiltonians.) Let us suppose we know the solution to this problem, so that the two arcs γ_1, γ_2 can be assumed to have the same end-points.

We now have to slide the interior of arc 1 onto arc 2. Classifying arcs with fixed end-points in a given

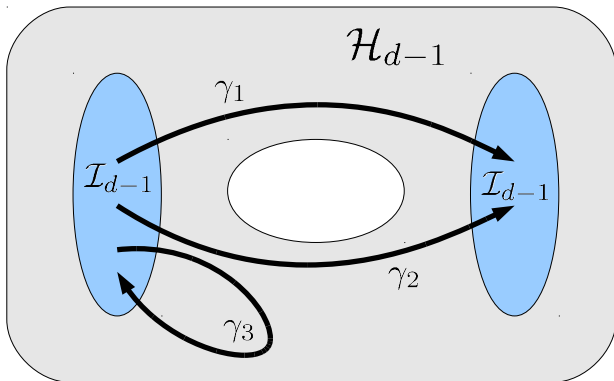


FIG. 3: Dimensional induction. The grey region represents \mathcal{H}_{d-1} : each point corresponds to a generic $d-1$ -dimensional Hamiltonian. The two ellipses on the side represent the components of \mathcal{I}_{d-1} , the oHamiltonians with inversion symmetry. Inversion-symmetric d -dimensional Hamiltonians (three of which are shown) are represented by arcs connecting points in \mathcal{I}_{d-1} . Two of these Hamiltonians are equivalent if the end-points are in the same component of \mathcal{I}_{d-1} and have the same winding numbers around holes in the space (represented by the white ellipse). For example, γ_2 and γ_3 are not equivalent because their final end-points are in different components; γ_1 and γ_2 are not equivalent because $\gamma_1\gamma_2^{-1}$ winds around the hole.

space is closely related to classifying closed loops. The *loops* in \mathcal{H}_2 can be classified by two winding numbers $\oint d\alpha(k_z)$ and $\oint d\beta(k_z)$, where α and β are angular variables around holes in \mathcal{H}_2 . This is a well-known result in disguise. Loops correspond to three-dimensional Hamiltonians without any special symmetry, which are classified (when there are sufficiently many bands) by three Chern numbers. The Chern number of the $k_z = 0$ cross-section is a function of the points in \mathcal{H}_2 , not of the loops, and it is constant for the whole component we are considering, so \tilde{G}_{Hz} does not matter. The remaining two Chern numbers are the winding numbers.

Now an arc connecting two points in \mathcal{H}_2 can wind around a hole in the space any number of times just like a loop; it just does not close on itself. The topology of loops is therefore determined by the value of $\int_0^\pi d\alpha(k_z)$ and $\int_0^\pi d\beta(k_z)$ as well.

The Chern numbers \tilde{G}_{Hx} and \tilde{G}_{Hy} of the full Hamiltonian are given by $\oint_{-\pi}^\pi d\alpha(k_z)$, $\oint_{-\pi}^\pi d\beta(k_z)$; hence the “winding numbers” of the open arcs are half as big as the Chern numbers, (by inversion symmetry). So if the Chern numbers of the arcs are equal the Hamiltonians are equivalent.

The only problem left is showing that the end-points can be slid to one another under appropriate conditions. This is the same as classifying inversion symmetric Hamiltonians in two-dimensions. This problem may be reduced to one dimension. The result is that, for two Hamiltonians in $k_x - k_y$ space to be equivalent, the Chern numbers \tilde{G}_{Hz} must be the same, and the one-dimensional boundary Hamiltonians must be equivalent.

Now we must classify inversion-symmetric Hamiltonians in one dimension. The problem reduces directly to zero dimensions because all one dimensional Hamiltonians without symmetry are equivalent.

Two zero-dimensional Hamiltonians (i.e., matrices!) are clearly equivalent if the numbers of even and odd occupied states are the same—just shift the energy eigenvalues so that the two Hamiltonians match. Hence the last condition is that the eight integers $n_o(\kappa)$ and the total number of occupied states n must match. (The original Hamiltonian has bifurcated into eight zero-dimensional Hamiltonians through the process of taking boundaries.) The number of even and odd unoccupied states above the Fermi energy must also be the same, but as mentioned above, there are an infinite number of these in continuous space.

Hence, three dimensional Hamiltonians are classified by \tilde{G}_{Hx} , \tilde{G}_{Hy} and \tilde{G}_{Hz} together with the parities at the TRIMs.

B. Constraint on Parities

Although the values of the 11 integers $n_o(\kappa)$ and \tilde{G}_{Hi} determine a phase, not all combinations of them are allowed. First of all, $\sum_{\kappa} n_o(\kappa)$ must be even (Eq. (4)). There are two ways to see this.

For the first explanation, let us understand a more general question: consider a Hamiltonian (not necessarily a gapped one) that is changing as a function of time. We will try to understand what happens when the parities at the TRIMs change. The parities at a TRIM change only when an even state at the TRIM below the Fermi energy and an odd state above the Fermi energy (or vice versa) pass through one another. Appendix B shows that, each time $n_o(\kappa)$ changes by 1 by means of such an interchange, a pair of Dirac points appears or disappears. Dirac points are defined as points where the valence and conduction bands cross, with a cone-shaped dispersion. They are stable unless they meet other Dirac points (with opposite “chirality”) and annihilate.

Now start from a trivial Hamiltonian, with all electrons glued to the Bravais lattice; in this Hamiltonian, all the parities are even. After an odd number of changes of $n_o(\kappa)$, there are an odd number of pairs of Dirac points, so the crystal is not insulating. If the system is insulating $\sum_{\kappa} n_o(\kappa)$ must be even.

The stability of the Dirac points is explained in part by the basic result on degeneracies of eigenvalues, rather than by symmetry: in order to tune a Hamiltonian to a point where there is a degeneracy, three parameters are sufficient. Since $H(\mathbf{k})$ is a function of three momenta, these may be tuned to a point where there is a degeneracy, provided H is close enough to having a degeneracy in the first place.

Any set of parities $n_o(\kappa)$ satisfying $\prod_{\kappa} \eta_{\kappa} = 1$ can be realized in an insulator. There is never a direct phase transition (even with fine tuning) between two such

phases when two or more $\eta_{\mathbf{k}}$'s flip sign. When two modes cross at one TRIM in order to change the value of n_o there, Dirac points will form, and the system will be a semimetal. The Dirac points must then move to the second TRIM and reannihilate, so that the system becomes an insulator again, as illustrated in Fig. 4

The alternative derivation of the constraint studies the Bloch eigenfunctions for a fixed Hamiltonian. Let us first suppose there is a single occupied band $|\psi_{1\mathbf{k}}\rangle$. To determine whether the wave function is even or odd, let us take its overlap with an even orbital $|s\rangle$ centered on the origin. Define $s_1(\mathbf{k}) = \langle s|\psi_{1\mathbf{k}}\rangle$. Plot the solutions in the Brillouin zone to

$$s_1(\mathbf{k}) = 0 \quad (14)$$

This equation is a complex equation, amounting to two equations in three variables, so its solutions are curves. At a TRIM, $\psi_{1\mathbf{k}}(\mathbf{r})$ is either even or odd. If it is odd, its overlap with $|s\rangle$ vanishes. Generically, the converse is also true. Hence, there is one curve through each TRIM where $|\psi_{1\mathbf{k}}\rangle$ is odd.

But since the curves are inversion symmetric, they must pass through an even number of TRIMs (see Fig. 5). Hence, the total number of TRIMs where $\mathcal{I}\psi_{1\mathbf{k}} = -\psi_{1\mathbf{k}}$ is even.

When there are several filled bands which do not touch each other, $\prod_{\mathbf{k}} \eta_a(\mathbf{k}) = 1$ for each band separately, and $\prod_{\mathbf{k}} \eta_{\mathbf{k}} = 1$ follows. If bands do touch, another step is required (the product for a single band may be -1 , but the total will still be $+1$). Consider the curves determined by $s_a(\mathbf{k}) = \langle s|\psi_{a\mathbf{k}}\rangle = 0$ for all the occupied bands $1 \leq a \leq n$. Some of these curves may be open arcs because $s_a(\mathbf{k})$ becomes discontinuous at Dirac points. Such arcs can only end at a Dirac point where the band touches another band. In this case, there is also an arc leaving the Dirac point in the other band (see App. C). Putting all the arcs from the occupied states together therefore produces a set of closed curves; these curves will be variegated if the arcs in each band are imagined to have different colors, but they are still closed. Hence we can still deduce that $\sum_{\mathbf{k}} n_o(\mathbf{k})$ is even.

C. Polarization and Hall Conductivity

The constraint just derived is not the only constraint on the 11 invariants. The parities of the $\tilde{\mathbf{G}}_H$ are determined by the parities of the n_o 's (see Eq. (5)). We will prove this momentarily, but it is logically necessary to derive the expression for the polarization first. Both these quantities are related to the Berry connection, a vector function in momentum space. For a single band, the Berry connection is defined by

$$\mathbf{A}_a(\mathbf{k}) = i\langle u_{a\mathbf{k}}|\nabla_{\mathbf{k}}|u_{a\mathbf{k}}\rangle \quad (15)$$

and the total Berry connection $\mathbf{A}(\mathbf{k})$ is the sum of the Berry connections of the occupied bands.

We will prove that the intrinsic polarization is given (modulo e times a lattice vector) by Eqs. (7),(8). In general, the polarization per unit cell is given by

$$\mathbf{P} = \mathbf{P}_e - \sum_i Z_i e(x_i - x_0). \quad (16)$$

The second term is the polarization of the nuclei in the unit cell relative to an origin, x_0 , and the first term is the polarization of the electrons relative to x_0 . Since the electrons are delocalized, calculating this contribution is subtle. It is given, according to Ref. 15, by

$$P_e = \frac{e}{2\pi} \sum_n \int dk A^n(k). \quad (17)$$

This expression for the polarization is ambiguous up to multiples of e , as it should be, on account of surface charge. If the unit cell is redefined, some nuclei locations are shifted by one unit. Likewise if the Bloch wave functions are redefined by $u_{nk} \rightarrow e^{i\theta(k)}u_{nk}$, then the polarization shifts by $\frac{e}{2\pi}(\theta(2\pi) - \theta(0))$, an integer multiple of e if $e^{i\theta}$ winds around the unit circle.

To evaluate the polarization of an insulator with inversion symmetry, set $x_0 = 0$, the inversion center. First, consider a single band. The wavefunctions at k and $-k$ must be the same up to a phase, so $\psi_{-k} = e^{i\theta(k)}\psi_k$ for some phase $\theta(k)$. Therefore, $A_k + A_{-k} = \theta'(-k)$. Combining k and $-k$ together in Eq. (17) leads to $\tilde{P}_e = \frac{1}{2\pi} \int_0^\pi \theta'(-k)dk = \frac{1}{2\pi}(\theta(-\pi) - \theta(0))$. Now $e^{i\theta(k)}$ is the parity of the wave function ± 1 at TRIMs $k = 0, \pi$. Hence if the parities at the TRIMs are different then the polarization is a half integer. If there are many bands, we may sum the polarization over all of them and we find in general that

$$(-1)^{2\tilde{P}_e} = \eta_0 \eta_\pi. \quad (18)$$

The result for the polarization in three dimensions is derived from this below, but Fig. 1d suggests the reason. Each of the four vertical lines through TRIMs looks like a one-dimensional insulator with half-integer polarization, so the net polarization per unit cell of the three-dimensional crystal is also $\frac{e}{2}\mathbf{R}_3$. Note that half of any Bravais lattice vector is an inversion center, so there are eight inequivalent inversion centers. The parities depend on which center they are measured relative to, so \mathbf{P}_e is origin-dependent. But \mathbf{P} is not because the contribution from the nuclei depends on the origin in the same way.

Now let us consider the Chern number for a *two* dimensional system, $H(k_x, k_y)$, and show that $(-1)^{\tilde{G}_{Hz}} = \prod_{\mathbf{k}} \eta_{\mathbf{k}}$. This is the two-dimensional version of Eq. (5). The Hamiltonian leads to a 1-D Hamiltonian H_{k_y} when k_y is fixed. As k_y changes, the polarization $P(k_y)$ of the one dimensional system changes. This means current must flow from one end to the other. According to Thouless's pumping argument, the Hall conductivity \tilde{G}_{Hz} is equal to the total charge (divided by e) that flows when k_y changes by 2π : (In real space, the one-dimensional

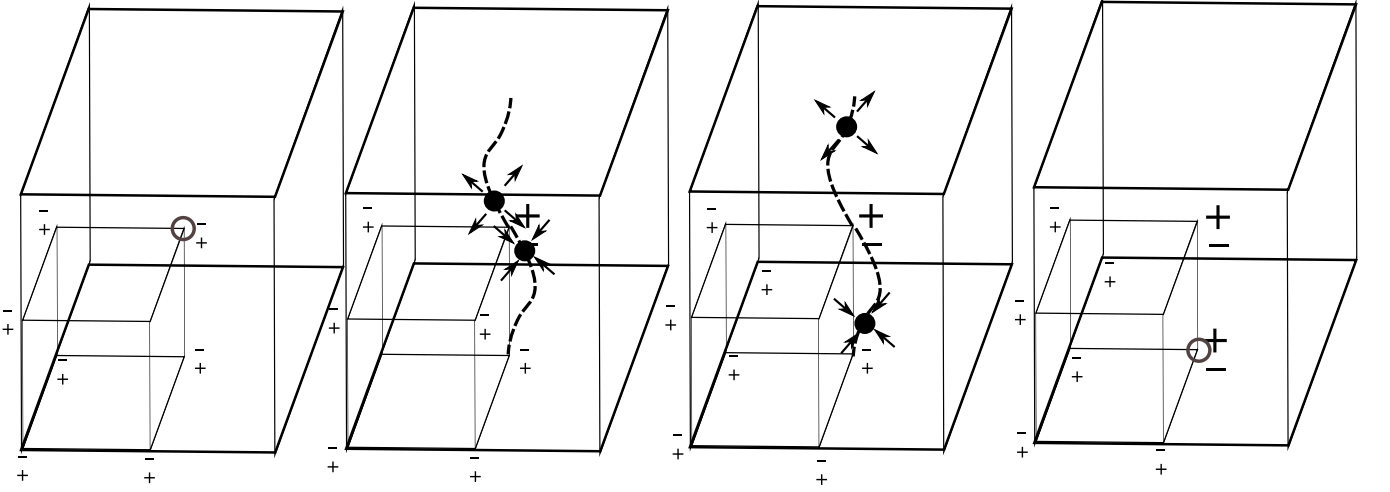


FIG. 4: Changing the parities of bands at two TRIMs. The figures represent the Brillouin zone of a system with two bands, one of which is filled. Initially, all the filled bands have parity +1, but the parities at two points are changed with the assistance Dirac points which also act as monopoles in the Berry flux (see appendix C). A pair of monopoles forms at one TRIM and they move to another TRIM where they annihilate. In the process, the parities of the states at both TRIMs are reversed. The open circles indicate where the monopoles start out and disappear.

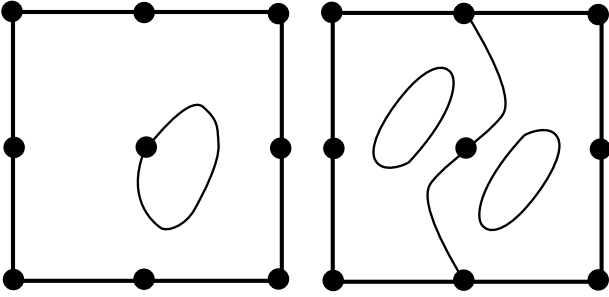


FIG. 5: Curves which are inversion symmetric must pass through an even number of TRIMs. Left, an attempt at drawing a curve that passes through one TRIM fails to be inversion symmetric. Right, an inversion symmetric figure; if there is just one curve passing through one of the TRIMs, it must go all the way around the Brillouin zone and pass through another TRIM on the way.

system is just the two-dimensional system rolled into a tube along the y direction, with period equal to a single cell. Changing k_y corresponds to applying an EMF around the y -direction.)

Thus $\tilde{G}_{Hz} = -\frac{1}{e} \int_{-\pi}^{\pi} dP(k_y)$. (The polarization is not single-valued if $\tilde{G}_z \neq 0$.) Now if $\prod_{\kappa} \eta(\kappa) = -1$ (as in either of the 2D layers in Fig. 1 b) then the polarizations at $k_y = 0$ and $k_y = \pi$ differ by a half integer. Thus, $\int_0^{\pi} dP = (k + \frac{1}{2})e$. By inversion symmetry, $dP(k_y) = dP(-k_y)$ (since $P(k_y + dk_y) - P(k_y) = -P(-k_y - dk_y) + P(-k_y)$). Hence between $-\pi$ and 0 the polarization changes by the same half-integer, and the full change in the polarization is odd, $\tilde{G}_{Hz} = -(2k + 1)2\pi$.

This section concludes with the generalizations of these results to three dimensions. The expression for the Hall

coefficient in three dimensions Eq. (5) is basically a restatement of the two-dimensional result. Each of the three components of \mathbf{G}_H is equal to the two-dimensional Hall coefficient for any cross-section of the Brillouin zone:

$$\begin{aligned} G_{Hz} &= \int \frac{dk_z}{(2\pi)} G_{Hz}^{2d}(k_z) \\ &= G_{Hz}^{2d}(k_{z0}) \end{aligned} \quad (19)$$

since the Chern number for any cross-section $k_z = k_{z0}$ is the same since it is a topological invariant.

The Hall coefficient can be obtained modulo 2 by looking at an inversion symmetric plane, either $k_z = 0$ or $k_z = \pi$, giving Eq. (5). Note that this gives another reason for the constraint $\prod_{\kappa} \eta_{\kappa} = 1$: the two planes have to agree about \tilde{G}_{Hz} 's parity.

The expression for the Hall coefficient can be guessed by looking at Fig. 4. The initial phase is trivial. When the monopoles move through the Brillouin zone and annihilate, they leave behind a magnetic flux, so the Chern number is 2π . The flux's direction is parallel to the edge where the parities of the occupied states have been flipped.

The polarization in three dimensions is well-defined if $\mathbf{G}_H = 0$; then there are no surface modes. According to Eq. 7, the pattern of signs is then a plane wave, so all the 1d polarizations at TRIMs, $P_{1d}^x(\kappa_y, \kappa_z)$, are the same. This value in fact coincides with the three dimensional polarization.

The three-dimensional polarization is the integral over one-dimensional polarizations, $P^x = \iint \frac{dk_y dk_z}{(2\pi)^2} P_{1d}^x(k_y, k_z)$, if $G_{Hy} = G_{Hz} = 0$. (This condition ensures that P^x is single-valued.) The integrand is not a constant, but by inversion symmetry $P_{1d}^x(k_y, k_z) - P_{1d}^x(0, 0) = -(P_{1d}^x(-k_y, -k_z) - P_{1d}^x(0, 0))$.

(Intuitively, one expects $P_{1d}^x(k_y, k_z)$ to be an odd function of the wave number, but only differences in polarization are inversion symmetric because of the ambiguity in the polarization.) Hence $P^x = P_{1d}^x(0, 0)$, which is given by Eq. (7) and Eq. (8).

Note that if \mathbf{G}_H is nonzero, then part of the polarization is still well-defined. If \mathbf{G}_H is parallel to \mathbf{g}_1 then *this* component of the polarization cannot leak through the surface modes. The chiral modes circle around the x -axis, so they do not provide a short circuit between the right and left faces of the crystal. In fact, the same reasoning shows that P_x is still given by Eqs. (7),(8).

D. Magnetoelectric Response

Now we justify the relation $\theta = \pi \frac{1}{2} \sum_{\kappa} n_o(\kappa)$ (Eq. (6)) by using the classification of topological insulators to deform an arbitrary inversion-symmetric Hamiltonian H to one that also has time-reversal symmetry. Eq. (6) is known for Hamiltonians with time-reversal in addition to inversion, either by directly evaluating the expression for θ in terms of the Berry connection⁹ or by combining the results of 6,7 and 8.

Hamiltonians with time-reversal symmetry and inversion symmetry have extra constraints on the $\tilde{\mathbf{G}}_H$ and n_o 's. The states at the TRIMs come in Kramers doublets, so $n_o(\kappa)$ and n are even, and the Hall conductivity must be 0 by symmetry. By the classification theory, an inversion symmetric insulator can be deformed into one that is also time-reversal symmetric if it has these properties, too, and Eq. (6) follows.

Now we are already assuming that the Hall conductivity is zero, since the gapless surface modes can interfere with the magnetoelectric response. When some of the n_o 's are odd there is an additional step before it is possible to deform H into a time-reversal symmetric Hamiltonian. We superimpose an independent inert system onto H and then deform the combined system. Consider an "ionic" or "frozen" insulator with protons on the Bravais lattice and electrons fixed on certain sites, and with all hopping amplitudes equal to zero. This insulator does not contribute to θ . If the electrons are at half of a Bravais lattice vector $\mathbf{p} = \frac{\mathbf{R}}{2}$ and its translates, then it is inversion symmetric.

Though this insulator does not contribute to θ , its parities depend on κ . This is enforced by Eq. (7) since the insulator has a polarization. Calculating these parities directly sheds light on Eq. (7). The parities are obtained by transforming to a basis of plane wave states,

$$|\mathbf{p}\rangle_{\mathbf{k}} = \sum_{\mathbf{R}} e^{i\mathbf{k} \cdot (\mathbf{R} + \mathbf{p})} |\mathbf{R} + \mathbf{p}\rangle \quad (20)$$

where $|\mathbf{r}\rangle$ represents an electron at an orbital centered around \mathbf{r} . When \mathbf{k} is a TRIM, $\mathcal{I}|\kappa\rangle_{\mathbf{p}} = e^{2i\mathbf{p} \cdot \kappa} |\kappa\rangle_{\mathbf{p}}$, assuming the orbitals are even under inversion.

Now consider an arbitrary Hamiltonian \mathcal{H} without Hall conductivity. Eq. (7) implies that the net parities $\eta(\kappa)$

vary just as they do in the ionic crystal (except possibly with an overall sign). Therefore, we can add a copy of an ionic crystal with a polarization that matches the intrinsic polarization of \mathcal{H} , leading to an extended Hamiltonian \mathcal{H}_{ext} . All the η_{κ} 's will become ± 1 . This sign can be changed to $+1$ —redefine the orbitals of the frozen crystal to be odd under inversion. (If *all* the signs were *initially* -1 add a frozen crystal with $\mathbf{p} = 0$ and odd parity orbitals.)

Now the $n_o(\kappa)$'s have become even. If n is odd then add an unpolarized crystal, with a single electron in an even orbital on the origin and its translates. Now both n and $n_o(\kappa)$ are both even.

This enlarged crystal's θ may be determined by deforming it to a time-reversal symmetric insulator, so $\frac{\theta_{\text{ext}}}{\pi} \equiv \frac{1}{2} \sum_{\kappa} n_{o,\text{ext}}(\kappa)$. But it has the same magnetoelectric response θ_{ext} as the original crystal, and the frozen crystals changed the number of odd states at the TRIMs by a multiple of 4; hence this formula applies to the original crystal also.

E. Other Quantized Responses?

We have found that there are eight integers $n_o(\kappa)$ that are constant within a given phase. However, the calculations so far have only found that a few mod. 2 combinations of them that have interpretations as response functions. We think that there are no quantized responses besides θ and \mathbf{G}_H , for any applied field or geometry. For any set of $n_o(\kappa)$'s, such that \mathbf{G}_H and θ are zero, it is possible to find a Hamiltonian where the particles have zero hopping.

Let us start from a general vector of values $n_o(\kappa)$ and try to build it out of the n_o vectors for the frozen (or ionic) insulators described in the previous section. Frozen insulators do not have any response. Regard $n_o(\kappa)$ as an eight-dimensional vector of integers \mathbf{n}_o . The vectors in this space can be pictured by labelling the vertices of a cube with eight numbers.

The frozen insulators described in the previous section give eight vectors $\mathbf{f}_{\mathbf{p}}$ in this space, as \mathbf{p} varies over all possible polarizations. (\mathbf{f}_0 represents the insulator where each $n_o = 1$.) Since \mathbf{n}_o is eight-dimensional and there are eight $\mathbf{f}_{\mathbf{p}}$'s, every insulator's vector can be decomposed in terms of these frozen vectors. This suggests that every insulator can be built out of frozen insulators. This is not really true though, because the superposition may involve non-integer coefficients. There is no way to take a fractional multiple of a system.

For each vector that *can* be expanded as $\mathbf{n}_o = \sum_{\mathbf{p}} r_{\mathbf{p}} \mathbf{f}_{\mathbf{p}}$ where the $r_{\mathbf{p}}$'s are integers, there is a frozen insulator with the same \mathbf{n}_o up to a constant. Hence these \mathbf{n}_o 's do not require nontrivial quantized responses. For each $\mathbf{p} \neq 0$, combine together $|r_{\mathbf{p}}|$ copies of the insulator with the polarization $\hat{\mathbf{P}}_e = \mathbf{p}$. (The parities of the inert orbitals should be chosen based on the sign of $r_{\mathbf{p}}$.)

How close can one get to a get \mathbf{n}_o can one get with

such a sum of frozen vectors? Appendix G shows that for each eight-component integer vector \mathbf{n}_o one can subtract a frozen vector \mathbf{f} so that

$$\mathbf{n}_o - \mathbf{f} = u_{xy}\mathbf{v}_{xy} + u_{xz}\mathbf{v}_{xz} + u_{yz}\mathbf{v}_{yz} + w_{xyz}\mathbf{v}_{xyz} \quad (21)$$

where the u 's are each 0 or 1 and \mathbf{w}_{xyz} is 0, 1, 2 or 3. The \mathbf{v} 's are the following vectors. The first, \mathbf{v}_{xy} corresponds to the insulator illustrated in Fig. 1b, with the quantum Hall response. It has ones on the *edge* of the cube described by $\kappa_x = \kappa_y = \pi$ and zeros everywhere else. The other v 's with two labels are defined symmetrically. The vector \mathbf{v}_{xyz} has a one at one *corner* of the cube ($\kappa_x = \kappa_y = \kappa_z = \pi$). If the vector \mathbf{n}_o of an insulator is decomposed in this way, the constraint $\sum_{\kappa} n_o(\kappa) \equiv 0 \pmod{2}$ implies that w_{xyz} is even (either 0 or 2 modulo 4). Hence the difference between a generic insulator and a frozen one is characterized by values of four numbers—each u can be 0 or 1 and w_{xyz} can be 0 or 2. Thus any property of the responses that is contained in the \mathbf{n}_o 's is determined by these four parameters.

Eqs. 21 and 5 show that the u 's describe the quantum Hall conductivity modulo 2, while $\theta = \pi$ if $\mathbf{G}_H = 0$ and $w_{xyz} \equiv 2 \pmod{4}$. There seem to be no other responses.

In spite of this, it is possible to measure some information about \mathbf{f} by considering the polarization. (The argument does not rule this out because polarization is static.)

IV. PARITIES AND THE ENTANGLEMENT SPECTRUM

The relations between the properties of the insulator and the parities can be derived geometrically using the entanglement spectrum of the insulator; there is a rule for counting the number of states in this spectrum based on the parities.

The entanglement spectrum is defined using the Schmidt decomposition. The insulator is cut by an imaginary plane passing through a center of inversion symmetry. The many-body ground state wave function then decomposes,

$$|\Psi\rangle = \frac{1}{\sqrt{Z}} \sum_{\alpha} e^{-\frac{E_{\alpha}^e}{2}} |\alpha\rangle_L |\alpha\rangle_R. \quad (22)$$

where Z is a normalization constant and E_{α}^e controls the weight of a given term. (It is called the entanglement “energy” because this formula looks similar to the Boltzmann distribution. The states can be called the entanglement states.)

When the wave function of the entire system is a Slater determinant, the entanglement states $|\alpha\rangle_L$ are Slater determinants, too²⁰. They are formed by selecting wave functions from a special family of single-particle wave functions $f_{i\mathbf{k}_{\perp}}^L(\mathbf{r})$. (These states may be labelled by the momentum along the surface, \mathbf{k}_{\perp} , by translational

symmetry.) Each of these wave-functions has an associated “energy” $\epsilon_{Li}(\mathbf{k}_{\perp})$ (as if they were eigenfunctions of a single-particle Hamiltonian). The entanglement “energy” E_{α}^e is the sum of all the “energies” of the occupied states. The entanglement spectra, $\epsilon_{Li}(\mathbf{k}_{\perp})$, can be used to determine “topological” properties of the system, since these spectra may be continuously deformed into the physical surface spectrum of the system^{11,12}.

Determining basic properties of the entanglement spectrum is simple in the presence of inversion symmetry. The entanglement spectrum has a particle-hole symmetry \mathcal{I}_e that implies a rule for finding the number of entanglement states at each surface TRIM. The \mathcal{I}_e symmetry takes each mode to another mode whose momentum \mathbf{k}_{\perp} and “energy” $\epsilon_i(\mathbf{k}_{\perp})$ have the opposite sign. Let us regard 0 as the Fermi “energy”; the state in the Schmidt decomposition with the smallest “energy” (i.e., the largest weight) is obtained by filling up all states with $\epsilon < 0$.

At surface TRIMs \mathcal{I}_e ensures that states appear in pairs with energies $\pm\epsilon$ when $\epsilon \neq 0$. There can be a single mode at zero. This mode will stay exactly at zero no matter how the system is changed, because moving away would break the symmetry. More can be said about the zero-energy states: the “index” at each TRIM can be determined; this is the difference $\Delta N_e(\kappa_{\perp})$ between the number of modes of even and odd parity. This quantity is significant because even and odd zero-energy states can “cancel” one another and move to nonzero energies $\pm\epsilon$, while two states of the same parity cannot. If two states evolve into the eigenstates f_1 and f_2 with energies of opposite sign, then f_1 and f_2 are orthogonal states exchanged by \mathcal{I}_e . The corresponding parity eigenstates, $\frac{1}{\sqrt{2}}(f_1 \pm f_2)$, have *opposite* parities.

The imbalance number can be found directly from the bulk band structure,

$$\Delta N_e(\kappa_{\perp}) = 1/2(\Delta N(\kappa_1) + \Delta N(\kappa_2)) \quad (23)$$

where κ_1 and κ_2 are the two bulk inversion-symmetric momenta that project to κ_{\perp} and $\Delta N(\kappa_1)$ (e.g.) is related to $n_o(\kappa_1)$; it is the difference between the number of even and odd occupied states at κ_1 , that is $n - 2n_o(\kappa_1)$. The parities of the bulk states are to be calculated relative to an inversion center that is on the cutting plane. (Parities depend on the inversion center, as does the entanglement spectrum. The physical responses described above do not.)

The derivation of this requires some results of Refs. 20,21 whose derivations are summarized in appendix D. As the structure of the entanglement spectrum suggests, the entanglement modes are actually eigenfunctions of a Hamiltonian H_L defined on the part of space to the left of the cutting plane. The eigenvalues of H_L are not equal to ϵ_i , but they are related to them,

$$H_L |f_{i\mathbf{k}_{\perp}}^L\rangle = \frac{1}{2} \tanh \frac{1}{2} \epsilon_{Li}(\mathbf{k}_{\perp}) |f_{i\mathbf{k}_{\perp}}^L\rangle.$$

The Hamiltonian H_L can be obtained from a Hamiltonian in the whole space, H_{flat} the flat-band Hamiltonian.

This Hamiltonian has the same eigenfunctions as the true Hamiltonian but has different eigenvalues, $-\frac{1}{2}$ for the occupied states and $+\frac{1}{2}$ for the empty ones. H_L is obtained from this by cutting off the right half of the space; cutting away the left half of the space leads to a partner Hamiltonian H_R (whose eigenfunctions f_R generate the Schmidt states on the right).

The flat-band Hamiltonian has an unusual property—its eigenstates can be reconstructed from the eigenstates of the two halves. There is a correspondence \mathcal{M} between the eigenfunctions of H_L and H_R which reverses the sign of the “energy”. Using this correspondence, define

$$F_{i\mathbf{k}_\perp}(\mathbf{r}) = \sqrt{\frac{1}{2} \operatorname{sech} \frac{\epsilon_{Li}(\mathbf{k}_\perp)}{2}} \times \left[e^{-\frac{1}{4}\epsilon_{Li}(\mathbf{k}_\perp)} f_{i\mathbf{k}_\perp}^L(\mathbf{r}) + e^{\frac{1}{4}\epsilon_{Li}(\mathbf{k}_\perp)} \mathcal{M} f_{i\mathbf{k}_\perp}^L(\mathbf{r}) \right]; \quad (24)$$

then F_{ik} is an eigenstate of H_{flat} with eigenvalue $-\frac{1}{2}$, and hence is occupied. As f_i^L varies over *all* eigenstates of H_L , the function F varies over a basis for the *occupied* states in the ground state²⁷

When the system is inversion symmetric, \mathcal{M} and \mathcal{I} can be combined together to give the symmetry \mathcal{I}_e ; it is a transformation within the left half of the insulator, defined by $\mathcal{I}_e = \mathcal{I}\mathcal{M}$. Since \mathcal{I} is a symmetry of the wave function, it preserves ϵ while \mathcal{M} reverses its sign. Therefore, \mathcal{I}_e acts as a particle-hole symmetry.

Now we return to the zero-“energy” states at TRIMs and their \mathcal{I}_e -parities $\eta_{ei\mathbf{k}_\perp}$. Each state $f_{i\mathbf{k}_\perp}$ extends, by Eq. (24), to an occupied state

$$F_{i\mathbf{k}_\perp} = \frac{1}{\sqrt{2}} \left[(f_{i\mathbf{k}_\perp}^L(\mathbf{r}) + \eta_{ei\mathbf{k}_\perp} f_{i\mathbf{k}_\perp}^L(-\mathbf{r})) \right]. \quad (25)$$

This state is invariant under \mathcal{I} , and the parity is $\eta_{ei\mathbf{k}}$.

Let us determine the value of ΔN_e for a one-dimensional system. The result in higher dimensions follows since we can use conservation of \mathbf{k}_\perp to reduce the dimension to 1. Consider a circular chain with an even number of cells, L . Now, count the number of even occupied states W_e minus the number of odd occupied states W_o , using two different bases. $W_e - W_o$ is equal to $\operatorname{tr} \mathcal{I}$ so it is basis independent.

One orthonormal basis will be obtained by cutting the system along a diameter. There will now be two cutting points 0 and $\frac{L}{2}$. The zero-“energy” states give parity eigenstates centered on each of the two cuts, according to Eq. (25). These contribute $2\Delta N_e$ to $W_e - W_o$. The remaining states can be organized into inversion-related pairs, $F_i(x), F_i(-x)$. All these states are mutually orthonormal because they correspond to different eigenvalues of H_L, H_R . The inversion matrix \mathcal{I} has only off-diagonal matrix elements between $F_i(\pm x)$, so they do not contribute to the trace.

On the other hand, instead of the localized wavefunctions, we can use the extended Bloch functions, $\psi_a(k_x)$. The wave functions at momentum $\pm k_x$ are exchanged, and the wave functions at the TRIMs contribute $\Delta N(\pi) + \Delta N(0)$ to $W_e - W_o$. Eq. (23) follows.

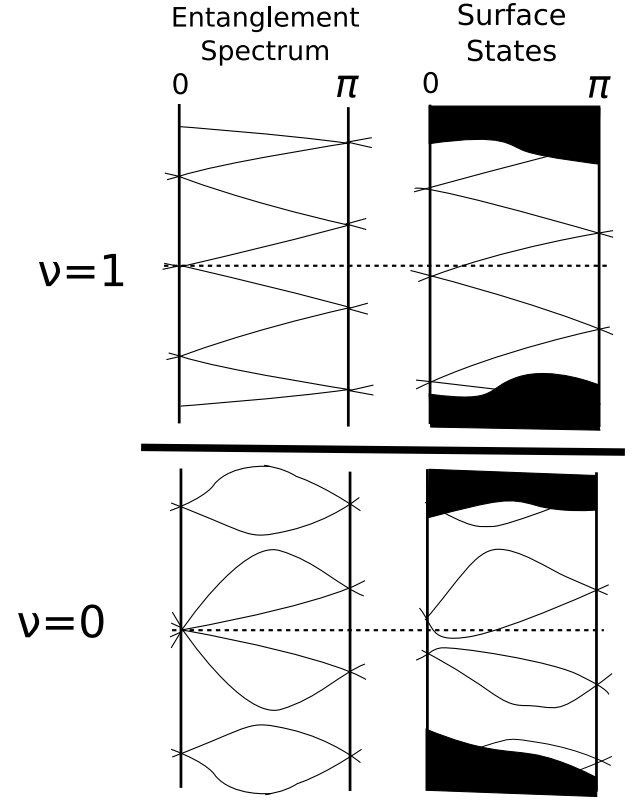


FIG. 6: Determining the Quantum Spin Hall index using the entanglement spectrum. The figure compares spectra of a nontrivial and a trivial system. The left spectrum for each system is the entanglement spectrum, and the right illustrates how the surface spectrum might look. In the entanglement spectrum, inversion symmetry protects degeneracies at zero energy at the TRIMs, allowing one to determine the index. But the two sets of spectra can be deformed into one another (the difference is probably more drastic than illustrated). Because time reversal symmetry produces Kramers degeneracies at the TRIMs at all energies, the parity of the number of modes crossing the Fermi energy does not change.

We can now count the edge states of a two-dimensional insulator that has both time reversal and inversion symmetry, to obtain the formulae from Ref. 8 for the indices of topological insulators. We will focus on the two dimensional quantum spin-Hall index, since the three dimensional indices are defined in terms of it. The quantum spin-Hall index ν is the number (modulo 2) of edge modes between 0 and π . Finding surface states in the entanglement spectrum is easy because of the extra particle-hole symmetry (see Fig. 6); these states remain when the spectrum is deformed into the physical spectrum, by the standard arguments.

Consider the entanglement spectrum created by dividing the system at $y = 0$. The index is the parity of the number of dispersion curves crossing a line $\epsilon = \text{const.}$ between $k_x = 0$ and π . Consider in particular the axis $\epsilon = 0$. Strictly between 0 and π the axis crosses an even number of modes: the crossings come in pairs because

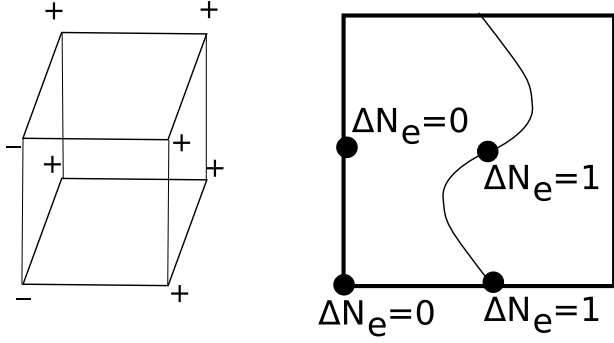


FIG. 7: A model with a single filled band that has an odd quantum Hall effect parallel to \mathbf{R}_z . a) The parities at the TRIMs. b) The entanglement states on the xz -face of the Brillouin zone, determined using $\Delta N_e(\boldsymbol{\kappa}_\perp) = \frac{1}{2}(\Delta N(\boldsymbol{\kappa}_1 + \Delta N(\boldsymbol{\kappa}_2))$.

the spectrum is symmetric under $\mathcal{T}\mathcal{I}_e$, which just flips the sign of ϵ . (Generically, these states will just mix and move off the axis.)

Therefore only the modes at the ends of the interval are important. We may assume that all the modes at either of these TRIMs have the same parity, because otherwise the states whose parity is in the minority may combine with the states in the majority and become gapped. Then by Eq. (23) the number of modes at, e.g., $k_x = 0$ is

$$|\Delta N_e(0)| = |n - n_o(0, 0) - n_o(0, \pi)|. \quad (26)$$

Since these modes are at the extremes of the interval from 0 to π , they only qualify as half-modes. One way to see this is to look at a line slightly above the axis. This line crosses half of the modes emanating from each TRIM, so the number of crossings, mod. 2, is $\nu \equiv \frac{1}{2} \sum_{k_x=0}^{\pi} |n - n_o(k_x, 0) - n_o(k_x, \pi)|$. This is congruent to $\frac{1}{2} \sum_{\boldsymbol{\kappa}} n_o(\boldsymbol{\kappa})$, summed over all four TRIMs.

When the flat band Hamiltonian is deformed into the true Hamiltonian, ν remains the same even though the surface states no longer have particle-hole symmetry. The energy curves form continuous loops or zigzags (see figure) because of the double-degeneracies protected by Kramers' theorem.

We can use a similar approach to understand the results for the polarization and Hall coefficient. These effects may be determined by sketching the arcs of the entanglement Fermi surface rather than the real one. While each zero energy state at a TRIM gives at least a Fermi point, not all of these points extend to Fermi arcs. It is certain that the *parity* of the number of Fermi arcs is the same as ΔN_e 's parity however. (This is proved in appendix E.)

Fig. 7 shows how the modes might look for a set of parities that corresponds to an odd quantum Hall conductance. Consider the xz surface of this insulator. According to Eq. (23) there must be one arc (or an odd number) passing through $(\pi, 0)$ and (π, π) , and an even number through the other two TRIMs. Hence as one

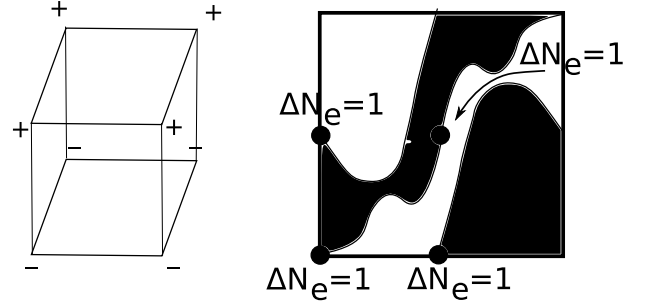


FIG. 8: Determining the polarization from the entanglement spectrum. a) Parities for an insulator with one filled band, with a half-filled Fermi sea in the entanglement spectrum. b) Possible entanglement Fermi arcs for a cut parallel to the xz plane. The arcs surround half the surface Brillouin zone. If there are no nuclei on $y = 0$, this crystal has a half-integer polarization in the y -direction.

travels along the x -direction through the Brillouin zone, one crosses an odd number of Fermi arcs. (Any extra arcs that do not pass through TRIMs come in pairs by inversion symmetry.) Since the number of arcs (counted with a sign depending on the sign of the group velocity) is the z -component of the Hall conductivity, $\tilde{G}_z/(2\pi)$ is odd.

Now consider the parities in Fig. 8. One possible choice of modes is illustrated. If these modes are not chiral, then the states below energy $\epsilon = 0$ cover half the Brillouin zone (exactly half because of the symmetry). This will imply that $P^y = \frac{\epsilon}{2}$ if there are no nuclei on $y = 0$.

The polarization is defined as the surface charge once the surface bands have been emptied. (See appendix F.) This definition may be applied to the entanglement spectrum. Cut the system with a plane $y = 0$ through a point of inversion symmetry. An important property of the entanglement spectrum is that every term in the Schmidt decomposition has a net charge of zero in the vicinity of the cutting surface.

Of all the terms in the Schmidt decomposition, consider the one with the largest coefficient, $|G\rangle_L |G\rangle_R$, where $|G\rangle_L$ and $|G\rangle_R$ are the ground states of H_L and H_R respectively, obtained by filling all the negative energy states. (It does not matter which of the states with exactly zero energy are filled.) These states are mirror images of each other, so they both have the same surface charge Q_y . The net charge is $2Q_y$. However, the Schmidt state $|G\rangle_L |G\rangle_R$, obtained by a hypothetical measurement of the two halves of the system, has the same charge as the ground state. Each electron is pushed over to the side of the $y = 0$ plane where it is more likely to be, but no electrons appear or disappear. Thus, $Q_y = 0$.

Now the ground state of H_L has a partially filled band. When this band (which covers half the Brillouin zone) is emptied, a charge of $-\frac{\epsilon}{2}$ per unit cell on the surface remains. Hence the polarization $P^y \equiv \frac{\epsilon}{2} \pmod{e}$.

To compare this result to Eq. (8), we need to take

nuclei into account. Note that $P_e^y = 0$ for the given parities. By neutrality, there must be a single charge $-e$ nucleus per unit cell, which contributes $P_n^y = -\frac{e}{2}$. Appendix F gives more details.

Conclusions This study of inversion symmetric insulators displays various interconnections between quantized electrical properties and the inversion parities at TRIMs. In particular, it provides a simple criterion for determining when a crystalline compound has a magnetoelectric response equal to π . The magnetoelectric effect could be seen in a system with broken time-reversal symmetry, even if the spin-orbit coupling is small.

The properties of inversion symmetric insulators can be derived in a simple way with the help of the entanglement spectrum.

Future work could extend these results to other interesting lattice symmetries, as well as the classification of superconductors with crystal symmetries. Finally, understanding the stability of the parity invariants to interactions will be an interesting subject for future study.

Acknowledgments This research was supported by NSF-DMR-0645691 and NSF-DMR-0804413. We thank Andrew Essin and Joel Moore for conversations about topological responses and Sergey Savrasov and Xiangang Wan for collaborating on a related project, thus helping to shape this article as well. Parallel work by T. Hughes, E.V. Prodan and B. A. Bernevig also considers inversion-symmetric insulators.

Appendix A: Classification using the topology of Hamiltonians

In this section we will show how to use systematic methods from topology to classify the insulators with inversion symmetry. This method was also used to find the phases of systems with one of the Altland and Zirnbauer symmetry groups^{2,3}.

In general we write a band insulator as $H(\mathbf{k})$, which we think of as a vector bundle on the Brillouin zone. The eigenvectors of $H(\mathbf{k})$ with energies below the chemical potential are the occupied states, defining a vector subspace of the entire Hilbert space at \mathbf{k} . For inversion-symmetric insulators, there is an additional constraint on the Hamiltonian: $\mathcal{P}^0[H(\mathbf{k})] \equiv I_0 H(\mathbf{k}) I_0 = H(-\mathbf{k})$, this relates the Hamiltonians at \mathbf{k} and $-\mathbf{k}$.

The idea behind our method of classification, similar to the one used for time-reversal invariant topological insulators, is to only look at half the Brillouin zone.

For a Hamiltonian H in d -dimensions, one can construct a path $f(t) = H(k_x = \pi t, k_2, k_3, \dots)$ in the space of $(d-1)$ -dimensional Hamiltonians, where the endpoints ($t = 0, 1$) are inversion symmetric. Thus the classification of d -dimensional Hamiltonians is equivalent to the classification of paths in $\mathfrak{P}(\mathcal{H}_{d-1}; \mathcal{I}_{d-1}, \mathcal{I}_{d-1})$, where \mathcal{H}_d is the set of general d -dimensional Hamiltonians and $\mathcal{I}_d \subset \mathcal{H}_d$ is the subset which is inversion-symmetric. The symbol

$\mathfrak{P}(X; A, B)$ is defined to be:

$$\begin{aligned} \mathfrak{P}(X; A, B) &\equiv \text{Set of paths in } X \text{ from } A \text{ to } B \quad (\text{A1}) \\ &= \{f : [0, 1] \rightarrow X | f(0) \in A, f(1) \in B\}, \end{aligned}$$

where $A, B \subset X$. We want to divide up \mathcal{I}_d into sets such that paths from different sets are not homotopic to each other. Heuristically, the classes of paths of $\mathfrak{P}(X; A, B)$ are given by the number of components of A, B which determines the set of possible endpoints, and the loop structure of X which determines the number of ways to travel from A to B . The classes of insulators in $d+1$ -dimensions is very roughly given by:

$$\begin{aligned} &\text{Components of } \mathcal{I}_{d+1} \\ &\sim \frac{\text{Loops in } \mathcal{H}_d}{\text{Loops in } \mathcal{I}_d} \times (\text{Components of } \mathcal{I}_d)^2. \quad (\text{A2}) \end{aligned}$$

This idea is made precise using algebraic topology²², and is captured by the exact sequence (A4).

There is an addition structure in the classification of insulators²², which comes from the fact that one can combine two insulators together using direct sums “ \oplus ”. To simplify the classification, it is useful to also have a subtraction “ \ominus ” operation between insulators. This would give the topological invariants (*e.g.* \mathbb{Z}) a group structure.

The subtraction procedure is realized by considering an ordered pair of bands (H_1, H_2) , which represents the “difference” of the two Hamiltonians. Addition by H' is given by $(H_1 \oplus H', H_2)$ and subtraction is given by $(H_1, H_2 \oplus H')$. Imposing the equivalence relation $(H_1 \oplus H', H_2 \oplus H') \sim (H_1, H_2)$ makes the addition and subtraction processes cancel each other. Physically, we are interested in classifying difference of two topological insulators – this is analogous to studying domain walls whose properties are determined only by the difference in topological invariants. With this interpretation, it is possible to talk about a negative number of filled bands (whenever H_2 has more bands than H_1).

The construction above, called the *Grothendieck group*, yields two direct results. First, two insulators H_1, H_2 are deformable to one another when the topological invariants of the band structure (H_1, H_2) are all trivial. Second, when the latter insulator is the vacuum, the topological invariants of (H, vac) are simply the bulk band invariants of H .

1. Hamiltonians, Classifying Spacing and Homotopy Groups

Consider an $N \times N$ matrix H with n occupied states and $N - n$ empty states. Setting the chemical potential to be zero, H is a matrix with n negative eigenvalues and $N - n$ positive eigenvalues. In the topological classification of insulators, the energies are irrelevant so long as we can distinguish between occupied and unoccupied states, and hence we can deform the energies (eigenvalues) of H .

all valence bands to -1 and the energies of conduction bands to $+1$. We can also assume there are an infinite number of conduction bands, and so we let $N \rightarrow \infty$. \mathcal{H}_0 is the set of such 0D Hamiltonians, and can be separated into discrete components based on the number of filled bands (which may be negative). The space \mathcal{H}_0 is homeomorphic to $\mathbb{Z} \times BU$, where BU is the classifying space of the unitary groups.

At the TRIM, the Hamiltonian is inversion-symmetric and commutes with the operator I_0 . The Hilbert space is divided into an even subspace and an odd subspace, based on the inversion eigenvalues. Hence the set of inversion-symmetric (0D) Hamiltonians \mathcal{I}_0 is homeomorphic to $\mathcal{H}_0 \times \mathcal{H}_0$.

Finally, we introduce the “vacuum” $v_0 \in \mathcal{I}_0 \subset \mathcal{H}_0$, which is a Hamiltonian with no filled bands. v_0 is a useful object in that it allows us to compare any Hamiltonian to it, and also acts as the basepoint when we compute the homotopy groups of $\mathcal{H}_0, \mathcal{I}_0$.

Given a topological space X and a basepoint within the space x_0 , the *homotopy group* $\pi_s(X)$ is the set of equivalence classes of maps $f : (S^s, b_0) \rightarrow (X, x_0)$, where the basepoint $b_0 \in S^s$ and $f(b_0) = x_0$. For example, $\pi_0(X)$ gives the number of connected components of X , $\pi_1(X)$ tells us which loops in X are equivalent and which loops are contractible.

The group structure of $\pi_s(X)$ is given by concatenation of maps. However, the group structure of the Hamiltonians has already been defined based on direct sums. Fortunately, the group composition defined based on the two methods (concatenation / direct sums) are compatible.

The homotopy groups of \mathcal{H}_d are known: $\pi_0(\mathcal{H}_0) = \mathbb{Z}$ because 0-dimensional Hamiltonians are classified by the number of filled bands n . $\pi_1(\mathcal{H}_0) = 0$ means that the loops in \mathcal{H}_0 are all contractible. $\pi_2(\mathcal{H}_0) = \mathbb{Z}$, because maps of the sphere are classified by the first Chern class (or the Chern number). This invariant give rise to the integer quantum Hall effect. For higher dimension, $\pi_s(\mathcal{H}_0)$ is 0 when s is an odd integer, and \mathbb{Z} when s is an even integer, corresponding to the $(s/2)^{\text{th}}$ Chern class. In this section, Chern numbers are taken to be integers rather than multiples of 2π .

The homotopy groups of \mathcal{I}_0 are simply the squares of the homotopy groups of \mathcal{H}_0 . In particular, the set of components $\pi_0(\mathcal{I}_0) = \mathbb{Z}^2$ is labeled by two integers: (n, α) , where n is the total number of valence “bands” and $\alpha = n_o$ is the number of states which have odd inversion parity.

2. Relative Homotopy Groups and Exact Sequences

The homotopy groups $\pi_s(X)$ classifies components, loops, and maps from higher dimensional spheres to the space X . The *relative homotopy groups* $\pi_s(X, A)$ classifies maps from paths, disks, *etc.* where the boundary

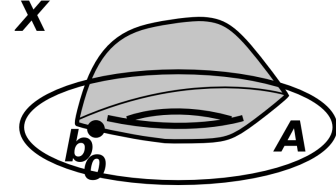


FIG. 9: Relative homotopy groups. The figure represents an element of $\pi_2(X, A, x_0)$ where X is \mathbb{R}^3 ; A is the torus.

must lie in some subspace (see Fig. 9). This is how topologists define “winding numbers” of open arcs, which were discussed in Sec. III A.

Given a space X a subspace $A \subset X$, and a basepoint $x_0 \in A$, the relative homotopy group $\pi_s(X, A)$ is the equivalence classes of maps $(D^s, \partial D^s, b_0) \rightarrow (X, A, x_0)$. The boundary of the disk $\partial D^s = S^{s-1}$ must map to A , and the basepoint $b_0 \in \partial D^s$ maps to x_0 . The relative homotopy groups can be computed via the exact sequence

$$\pi_s(A) \xrightarrow{i_*} \pi_s(X) \xrightarrow{j_*} \pi_s(X, A) \xrightarrow{\partial} \pi_{s-1}(A) \xrightarrow{i_*} \pi_{s-1}(X). \quad (\text{A3})$$

An *exact sequence* is a sequence of groups along with maps defined from one group to the next, each map preserving the group operations. In an exact sequence, the image of every map is the same as the kernel of the subsequent map.

In the one-dimensional case, the relative homotopy group $\pi_1(X, A)$ describes the set of possible paths in X from x_0 to A up to homotopy, that is, the classes of paths $\mathfrak{P}(X; x_0, A)$. The exact sequence becomes:

$$\pi_1(A) \xrightarrow{i_{(1)}} \pi_1(X) \xrightarrow{j_{(1)}} \pi_1(X, A) \xrightarrow{\partial} \pi_0(A) \xrightarrow{i_{(0)}} \pi_0(X). \quad (\text{A4})$$

In the exact sequence above, the maps are defined as follows.

- $i : A \rightarrow X$ is the inclusion map which takes every point from A to a point in X . The induced maps $i_{(s)} : \pi_s(A) \rightarrow \pi_s(X)$ and takes components/loops from one space to the other.
- All the loops in X start and end at x_0 , and so they are also clearly paths in $\mathfrak{P}(X; x_0, A)$ seeing $x_0 \in A$. $j_{(1)}$ is the map that takes the equivalence classes of loops $\pi_1(X)$ to the equivalence classes of paths $\pi_1(X, A)$.
- $\partial : \pi_1(X, A) \rightarrow \pi_0(A)$ is a map that takes a path and selects its endpoint to give a component of A . ∂ is called the boundary map, it takes a “1D object” to give a “0D object.”

It appears that the maps i and j “do nothing” to the objects (points, loops) they act on. However, each map gives the loop/path more freedom to move around. For

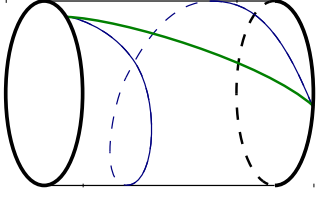


FIG. 10: Understanding the exact sequence. Paths in $\pi_1(X, A)$ can be enumerated by taking one path for each inequivalent end-point and adding loops from $\pi_1(X)$ to the paths. This description is sometimes redundant. In this figure, X is the cylinder and A is the two circles at its ends. A path p and a path $p' = p + l$ obtained from it are shown where l winds around the cylinder. The two paths are equivalent because they can be deformed into one another by bringing the right end-point around A . This happens because l can be smooshed into A .

example, $j_{(1)}$ takes a loop to a path where the endpoints no longer have to be the same.

The exact sequence captures the idea that the paths in $\mathfrak{P}(X; x_0, A)$ can be classified once one knows the properties of X and A , based on their end-points and how they wind.

1. First, we pick the endpoint $x \in A$ of the path p . x must be connected to x_0 . and this is captured by the statement $\ker(i_{(0)}) = \text{img}(\partial)$. The explanation is as follows. The endpoint of the path is given by the ∂ map: $x = \partial p$. The image of ∂ is thus the set of elements of $\pi_0(A)$ that are connected to x_0 within X . On the other hand, these are exactly the components which become equal to 0 in $\pi_0(X)$, when A is enlarged. Hence $\ker(i_{(0)}) = \text{img}(\partial)$.
2. Given a choice of a path p from x_0 to x , we can construct all the other paths between the points. We can create any other path p' by concatenating a loop $l \in \pi_1(X)$ at the beginning of p .
3. However, the paths p and p' are only different (*i.e.* not homotopic to each other) only if the loop l cannot be unwound within A , this is to say that $p \sim p'$ if l is homotopic to a loop in A . See Fig. 10. This idea is captured by the exactness at $\pi_1(X)$. Hence we think of l belonging to the quotient $\frac{\pi_1(X)}{i_{(1)}\pi_1(A)}$, and this group is called the *cokernel* of the map $i_{(1)}$.

We see that any path may be constructed by its endpoint x and a loop l .

$$p = j(l) + \partial^{-1}x. \quad (\text{A5})$$

The inverse boundary operator ∂^{-1} is not unique, but that does not affect the structure of the group $\pi_1(X, A)$ for the cases we are considering. The equivalence classes of x form $\ker(i_{(0)})$, while the equivalence classes of l make

up $\text{coker}(i_{(1)})$. The relative homotopy group is a semidirect product

$$\pi_1(X, A) = \text{coker}(i_{(1)}) \rtimes \ker(i_{(0)}). \quad (\text{A6})$$

What this means is that $\text{coker}(i_{(1)})$ is a normal subgroup of $\pi_1(X, A)$ and $\ker(i_{(0)})$ is the quotient of the two. For the purpose of classifying inversion-symmetric insulators, we can treat the semidirect product as simply a product.

3. One Dimension

In this section we examine the classification of 1D inversion-symmetric Hamiltonians $H(k)$. Let \mathcal{I}_1 be the set of maps $H : S^1 \rightarrow \mathcal{H}_0$ such that $\mathcal{P}^0[H(k)] = H(-k)$. \mathcal{I}_1 is homeomorphic to the set of paths in \mathcal{H}_0 that start and end in \mathcal{I}_0 (*i.e.* $\mathcal{I}_1 \approx \mathfrak{P}(\mathcal{H}_0; \mathcal{I}_0, \mathcal{I}_0)$), and we seek to classify all such paths - to compute $\pi_0(\mathcal{I}_1)$.

For a 1D band structure $H(k)$, we can ‘factor’ out $H(0)$ by letting $H'(k) = H(k) \ominus H(0)$ such that $H'(0) = v_0$. $H(0)$ is an element of \mathcal{H}_0 while $H'(k)$ is an element of $\tilde{\mathcal{I}}_1$, where $\tilde{\mathcal{I}}_1$ is the subset of \mathcal{I}_1 with a fixed basepoint ($H'(0) = v_0$). The decomposition $H(k) = H(0) \oplus H'(k)$ can be expressed as

$$\mathcal{I}_1 = \mathcal{I}_0 \times \tilde{\mathcal{I}}_1. \quad (\text{A7})$$

Hence the classification of \mathcal{I}_1 can be broken up in to two parts, the classification of \mathcal{I}_0 and that of $\tilde{\mathcal{I}}_1$. The former is understood as $\pi_0(\mathcal{I}_0) = \mathbb{Z}^2$.

Notice that $\tilde{\mathcal{I}}_1$ is homeomorphic with the class of paths $\mathfrak{P}(\mathcal{H}_0; v_0, \mathcal{I}_0)$, whose components are described by the relative homotopy group $\pi_1(\mathcal{H}_0, \mathcal{I}_0)$. These correspond to the possible phases of band structures in $\tilde{\mathcal{I}}_1$. The relative homotopy group can be computed by the exact sequence (A4). Using the fact that $\pi_0(\tilde{\mathcal{I}}_1) = \pi_1(\mathcal{H}_0, \mathcal{I}_0)$,

$$\begin{array}{ccccccc} \pi_1(\mathcal{I}_0) & \xrightarrow{i_*^1} & \pi_1(\mathcal{H}_0) & \xrightarrow{j_*^0} & \pi_0(\tilde{\mathcal{I}}_1) & \xrightarrow{\partial} & \pi_0(\mathcal{I}_0) \xrightarrow{i_*^0} \pi_0(\mathcal{H}_0) \\ 0 & & 0 & & & & \mathbb{Z}^2 \quad \mathbb{Z} \end{array} \quad (\text{A8})$$

Since $\pi_1(\mathcal{H}_0) = 0$, we can ignore the left side of the exact sequence (cokernel of $i_{(1)}$ is zero). The integer $n \in \pi_0(\mathcal{H}_0) = \mathbb{Z}$ tells us how many filled bands there are, and $(n_o, n_e) \in \pi_0(\mathcal{I}_0) = \mathbb{Z}^2$ are the number of even-parity and odd-parity bands. The map $i_{(0)}$ is given by $n = n_o + n_e$, and so the kernel of the map is the subset where $n_o = -n_e$, isomorphic to \mathbb{Z} .²⁸ It is clear that $\pi_0(\tilde{\mathcal{I}}_1)$ is isomorphic to $\ker(i_{(0)}) = \mathbb{Z}$. This is to say that the set of paths $\mathfrak{P}(\mathcal{H}_0; v_0, \mathcal{I}_0)$ are solely classified by the endpoint. Since $\mathcal{I}_1 = \mathcal{I}_0 \times \tilde{\mathcal{I}}_1$, we have

$$\begin{aligned} \pi_0(\mathcal{I}_1) &= \pi_0(\mathcal{I}_0) \times \pi_0(\tilde{\mathcal{I}}_1) \\ &= \pi_0(\mathcal{I}_0) \times \pi_1(\mathcal{H}_0, \mathcal{I}_0) \\ &= \mathbb{Z}^2 \times \mathbb{Z}. \end{aligned} \quad (\text{A9})$$

The invariant $\pi_0(\mathcal{I}_0) = \mathbb{Z}^2$ corresponds to the number of total bands and odd-parity states at $k = 0$: $n, n_o(0)$.

The invariant $\pi_0(\tilde{\mathcal{I}}_0) = \mathbb{Z}$ corresponds to the difference in number of odd bands at $k = \pi$ and $k = 0$: $\alpha_x = n_o(\pi) - n_o(0)$. Hence the parities at the two TRIMs completely classify all 1D inversion-symmetric Hamiltonians.

A *generator* of a group is an element which gives the entire group by group addition and subtraction, for example 1 is a generator of \mathbb{Z} . In our case, the generators are Hamiltonians which forms a basis for all Hamiltonians, up to homotopy.

The generators of $\pi_0(\mathcal{I}_0) = \mathbb{Z}^2$ are two Hamiltonians H_n^0 and H_α^0 which adds one even-parity and odd-parity band to the system, respectively. Explicitly:

$$H_n^0 = [-1]_{(+)} \cdot \quad (\text{A10})$$

$$H_\alpha^0 = [-1]_{(-)} \ominus H_n^0. \quad (\text{A11})$$

where the subscript (\pm) labels the inversion eigenvalue(s) of the orbital(s). The first expression H_n^0 adds an inert band to increase n ; the second expression H_α^0 adds an odd-parity band but subtracts an even-parity one to increase n_o while maintaining n . The generator for $\pi_0(\tilde{\mathcal{I}}_1) = \mathbb{Z}$ is:

$$H_\alpha^1(k) = \begin{bmatrix} -\cos k & \sin k \\ \sin k & \cos k \end{bmatrix}_{(+)} \ominus H_n^0. \quad (\text{A12})$$

The subscript $(+-)$ specifies the inversion operator $I_0 = \begin{bmatrix} +1 & -1 \\ -1 & +1 \end{bmatrix}$ for this Hamiltonian. When $k = 0$, the matrix becomes $\begin{bmatrix} -1 & 1 \\ 1 & -1 \end{bmatrix}_{(+-)}$ and the occupied band is even under inversion. Similarly, the matrix at $k = \pi$ is $\begin{bmatrix} 1 & -1 \\ -1 & 1 \end{bmatrix}_{(+-)}$ and there the occupied band is odd. Hence $\alpha_x = n_o(\pi) - n_o(0) = 1 - 0 = 1$ and $H_\alpha^1(k)$ is a generator of $\pi_0(\tilde{\mathcal{I}}_1)$.

Therefore, any 1D inversion-symmetric Hamiltonian is homotopic to

$$H(k) = nH_n^0 \oplus \alpha H_\alpha^0 \oplus \alpha_x H_\alpha^1(k). \quad (\text{A13})$$

4. Two Dimensions

We apply the same ideas used in 1D to classify inversion-symmetric insulators in 2D. The inversion-symmetric Hamiltonians (k_x, k_y) in 2D satisfy: $\mathcal{P}^0 H(k_x, k_y) = H(-k_x, -k_y)$. The set of 2D inversion symmetric Hamiltonians (\mathcal{I}_2) is equivalent to $\mathfrak{P}(\mathcal{H}_1; \mathcal{I}_1, \mathcal{I}_1)$, where \mathcal{H}_1 is the set of 1D band structures (loops in \mathcal{H}_0).

Just as in the 1D case where we decompose $H(k)$ into a 0D and 1D object: $H(k) = H(0) \oplus H'(k)$, we decompose the 2D Hamiltonian into 0D, 1D and 2D components. Let

$$H'(k_x, k_y) = H(k_x, k_y) \ominus H(0, 0), \quad (\text{A14a})$$

so that $H'(0, 0) = v_0$. Now we define

$$H''(k_x, k_y) = H'(k_x, k_y) \ominus H'(0, k_y) \ominus H'(k_x, 0), \quad (\text{A14b})$$

so that

$$H''(0, k_y) = H''(k_x, 0) = v_0. \quad (\text{A15})$$

$H(0, 0)$ is an element of \mathcal{I}_0 , and $H'(0, k_y)$ and $H'(k_x, 0)$ are elements of $\tilde{\mathcal{I}}_1$. We define $\tilde{\mathcal{I}}_2$ to be the set of inversion-symmetric Hamiltonians satisfying (A15). With this procedure, we have decomposed \mathcal{I}_2 as

$$\mathcal{I}_2 = \tilde{\mathcal{I}}_0 \times \tilde{\mathcal{I}}_1^2 \times \tilde{\mathcal{I}}_2, \quad (\text{A16})$$

where $\tilde{\mathcal{I}}_0 = \mathcal{I}_0$. Explicitly, the decomposition is:

$$\begin{aligned} H(k_x, k_y) &= \underbrace{H(0, 0)}_{\tilde{\mathcal{I}}_0} \oplus \underbrace{H'(0, k_y) \oplus H'(k_x, 0)}_{\tilde{\mathcal{I}}_1 \times \tilde{\mathcal{I}}_1} \oplus \underbrace{H''(k_x, k_y)}_{\tilde{\mathcal{I}}_2} \end{aligned} \quad (\text{A17})$$

Due to (A15), we can think of Hamiltonians in $\tilde{\mathcal{I}}_2$ as maps from the sphere (rather than the torus) to \mathcal{H}_0 .

We now analyze the properties of Hamiltonians in $\tilde{\mathcal{I}}_2$. For each fixed k_x , the Hamiltonian $H''(k_y)|_{k_x}$ is a map from the 1D Brillouin zone (S^1) to $\tilde{\mathcal{H}}_0$ (where we've also defined $\tilde{\mathcal{H}}_0 = \mathcal{H}_0$). Denote the set of such maps as $\tilde{\mathcal{H}}_1$, the set of loops in $\tilde{\mathcal{H}}_0$ with basepoint v_0 : $\tilde{\mathcal{H}}_1 = \mathfrak{P}(\tilde{\mathcal{H}}_0; v_0, v_0)$. $\tilde{\mathcal{H}}_1$ is called the *loop space* of $\tilde{\mathcal{H}}_1$, and the notation used in literature is $\tilde{\mathcal{H}}_1 = \Omega\tilde{\mathcal{H}}_0$.

The Hamiltonian at $k_x = \pi$ is inversion-symmetric, and so $H''(k_y)|_{k_x=\pi} \in \tilde{\mathcal{I}}_1$. At $k_x = 0$, the line $H''(k_y)|_{k_x=0} = v_0$ is a constant map - which we call v_1 (a line of v_0). Clearly v_1 is an element of $\tilde{\mathcal{I}}_1$, and acts as the basepoint when we compute the homotopy groups of $\tilde{\mathcal{I}}_1, \tilde{\mathcal{H}}_1$.

Having defined the spaces $\tilde{\mathcal{I}}_2, \tilde{\mathcal{H}}_1$ and basepoint v_1 , we can see that $\tilde{\mathcal{I}}_2$ is homeomorphic to the set of paths in $\tilde{\mathcal{H}}_1$ with endpoints at v_1 and $\tilde{\mathcal{I}}_1$: $\tilde{\mathcal{I}}_2 \approx \mathfrak{P}(\tilde{\mathcal{H}}_1; v_1, \tilde{\mathcal{I}}_1)$. The exact sequence which gives the equivalence classes of such paths is

$$\pi_1(\tilde{\mathcal{I}}_1) \xrightarrow{i_*^1} \pi_1(\tilde{\mathcal{H}}_1) \xrightarrow{j_*^1} \pi_0(\tilde{\mathcal{I}}_2) \xrightarrow{\partial} \pi_0(\tilde{\mathcal{I}}_1) \xrightarrow{i_*^1} \pi_0(\tilde{\mathcal{H}}_1). \quad (\text{A18})$$

Elements of $\pi_1(\tilde{\mathcal{H}}_1)$ are two-dimensional Hamiltonians that equal v_0 along $k_x = 0 \sim 2\pi$ and $k_y = 0 \sim 2\pi$, which are equivalent to maps $S^2 \rightarrow \tilde{\mathcal{H}}_0$. Hence

$$\pi_1(\tilde{\mathcal{H}}_1) = \pi_2(\tilde{\mathcal{H}}_0) = \mathbb{Z} \quad (\text{Chern number}). \quad (\text{A19})$$

The map j^1 , which essentially maps general two-dimensional Hamiltonians to inversion symmetric ones, is defined by

$$\begin{aligned} (j^1 H)(k_x, k_y) &= \begin{cases} H(2k_x, k_y) & 0 \leq k_x \leq \pi \\ \mathcal{P}^0 H(4\pi - 2k_x, 2\pi - k_y) & \pi \leq k_x < 2\pi \end{cases} \end{aligned} \quad (\text{A20})$$

It builds an inversion symmetric Hamiltonian out of two copies of a Hamiltonian with no special symmetries. The map $\partial: \tilde{\mathcal{I}}_2 \rightarrow \tilde{\mathcal{I}}_1$ is defined by

$$[\partial H](k) = H(k_x = \pi, k_y = k) \quad (\text{A21})$$

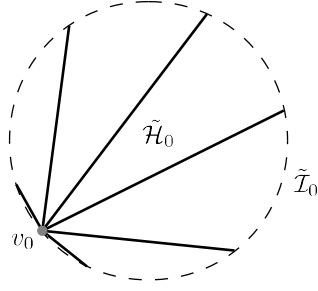


FIG. 11: Isomorphism between $\pi_2(\tilde{H}_0, \tilde{I}_0)$ and $\pi_1(\tilde{I}_1)$. An element in \tilde{I}_1 is a path from v_0 to an element of \tilde{I}_0 (dark black lines). An element of $\pi_1(\tilde{I}_1)$ is a family of such paths. The first path in the family must be v_1 , a “zero-length” constant path at v_0 (gray dot). The last path of the family must also be v_1 , and so the paths must shrink back to v_0 at the end, because that is the base point for the homotopy groups. This family of paths traces out a disk D^2 which maps to \tilde{H}_0 , the endpoints of each path traces out a circle $S^1 = \partial D^2$ which maps to \tilde{I}_0 (dashed circle). The basepoint of the circle maps to v_0 , and hence every element of $\pi_1(\tilde{I}_1)$ is also an element of $\pi_2(\tilde{H}_0, \tilde{I}_0)$ and vice-versa. This establishes the isomorphism $\pi_2(\tilde{H}_0, \tilde{I}_0) = \pi_1(\tilde{I}_1)$.

which takes a 2D Hamiltonian and picks out the 1D Hamiltonian at $k_x = \pi$.

To solve the exact sequence earlier (A18), we need to compute $\pi_1(\tilde{I}_1)$, which classifies loops of 1D inversion-symmetric insulators (not to be confused with 2D insulators). As argued in Fig. 11, the group $\pi_1(\tilde{I}_1)$ is isomorphic to $\pi_2(\tilde{H}_0, \tilde{I}_0)$. We can compute $\pi_1(\tilde{I}_1) = \pi_2(\tilde{H}_0, \tilde{I}_0)$ via the exact sequence (A3).

$$\begin{array}{ccccccc} \pi_2(\tilde{I}_0) & \xrightarrow{i_*^0} & \pi_2(\tilde{H}_0) & \xrightarrow{j_*^0} & \pi_1(\tilde{I}_1) & \xrightarrow{\partial} & \pi_1(\tilde{I}_0) \xrightarrow{i_*^0} \pi_1(\tilde{H}_0) \\ \mathbb{Z}^2 & & \mathbb{Z} & & & & 0 \\ & & & & & & 0 \end{array} \quad (\text{A22})$$

The first map $i_{(2)}^0 : \pi_2(\tilde{I}_0) \rightarrow \pi_2(\tilde{H}_0)$ is given by $\beta = \beta_e + \beta_o$ (which means that the Chern numbers of the odd and even bands add to the total.) The image of $i_{(2)}^0$ is all of $i_{(2)}^0$, so its cokernel is trivial. Since on the right side the groups are also trivial ($\ker(i_{(1)}^0) = 0$), we have that $\pi_1(\tilde{I}_1) = 0$.

We now return to the exact sequence (A18) to compute the $\pi_0(\tilde{I}_2)$.

$$\begin{array}{ccccccc} \pi_1(\tilde{I}_1) & \xrightarrow{i_*^1} & \pi_0(\tilde{H}_2) & \xrightarrow{j_*^1} & \pi_0(\tilde{I}_2) & \xrightarrow{\partial} & \pi_0(\tilde{I}_1) \xrightarrow{i_*^1} \pi_0(\tilde{H}_1) \\ 0 & & \mathbb{Z} & & & & 0 \end{array} \quad (\text{A23})$$

The exact sequence yields $\pi_0(\tilde{I}_2) = \mathbb{Z} \times \mathbb{Z}$; the set of $H''(\mathbf{k})$ are classified by two integers $(\alpha_{xy}, \beta_{xy})$. The first integer α_{xy} coming from the map ∂ gives $n_o(\pi, \pi)$; the second integer β_{xy} is related to the Chern number of H'' . The basis of $\pi_0(\tilde{I}_2)$ are found by taking the image of the generator in $\pi_1(\tilde{H}_1)$ and one of the preimages of the

generator element in $\pi_0(\tilde{I}_1)$, which we denote by $H_\beta^2(\mathbf{k})$ and $H_\alpha^2(\mathbf{k})$ respectively. Any Hamiltonian in \tilde{I}_2 , up to a homotopy, can be written as

$$H'' = \beta_{xy} H_\beta^2 \oplus \alpha_{xy} H_\alpha^2. \quad (\text{A24})$$

The generator $H_\beta^2(\mathbf{k}) = i_{(1)}^1 H_{\text{chern}}(\mathbf{k})$ where H_{chern} is the generator of $\pi_1(\tilde{H}_1) = \pi_2(\tilde{H}_0)$, *i.e.* a 2D band insulator with Chern number +1. $H_\alpha^2(\mathbf{k})$ is defined such that $(\partial H_\alpha^2)(k) = H_\alpha^1(\pi, k)$ is the 1D insulator (A12).

Explicitly, the generator

$$H_\alpha^2(\mathbf{k}) = \frac{1}{1+x^2+y^2} \begin{bmatrix} 1-x^2-y^2 & 2(y+ix) \\ 2(y-ix) & x^2+y^2-1 \end{bmatrix}_{(+ -)}, \quad \ominus H_n^0, \quad (\text{A25})$$

where $x = \cot \frac{k_x}{2}, y = \cot \frac{k_y}{2}$. When x or $y = 0$, then $x^2 + y^2 \rightarrow \infty$ and $H_\alpha^2(\mathbf{k}) = \begin{bmatrix} -1 & \\ & 1 \end{bmatrix}_{(+ -)}$ and $n_o(\mathbf{k}) = 0$. When $x = y = \pi$, it can be seen that $H_\alpha^2(\mathbf{k}) = \begin{bmatrix} 1 & \\ & -1 \end{bmatrix}_{(+ -)}$ and the filled band is odd under inversion. Note that the Hamiltonian has Chern number +1. Since $\alpha_{xy} = n_o(\pi, \pi)$ (and the other TRIMs have $n_o = 0$ because of the normalization), this is related to the constraint $\tilde{G} \equiv \sum_{\kappa} n_o(\kappa)$.

The other generator $H_\beta^2(\mathbf{k}) = i_{(1)}^1 H_{\text{chern}}(\mathbf{k})$:

$$H_\beta^2(k_x, k_y) = H_\alpha^2(2k_x, k_y). \quad (\text{A26})$$

has Chern number +1 in each of the halves $0 \leq k_x \leq \pi$ and $\pi \leq k_x \leq 2\pi$. Evidently, the Chern number of the entire Brillouin zone is given by

$$\tilde{G} = \alpha_{xy} + 2\beta_{xy}, \quad (\text{A27})$$

since H_α^2, H_β^2 has Chern number 1, 2 respectively.

The decomposition (A16) gives us six \mathbb{Z} invariants in 2D: two from \tilde{I}_0 , one from each of the two \tilde{I}_1 , and two more from \tilde{I}_2 . The six invariants $(n, \alpha, \alpha_x, \alpha_y, \alpha_{xy}, \beta_{xy})$ are related to the properties of the original Hamiltonian $H(k_x, k_y)$ as follows:

- n gives the number of filled bands, generated by (A10).
- $\alpha = n_o(0, 0)$ is the number of odd-parity states at $(k_x, k_y) = (0, 0)$, generated by (A11).
- $\alpha_x = n_o(\pi, 0) - n_o(0, 0)$ involves the difference between two parities, generated by (A12) ($k \rightarrow k_x$).
- $\alpha_y = n_o(0, \pi) - n_o(0, 0)$ involves the difference between two parities, generated by (A12) ($k \rightarrow k_y$).
- $\alpha_{xy} = n_o(\pi, \pi) - n_o(\pi, 0) - n_o(0, \pi) + n_o(0, 0)$ involves the parities at all TRIMs, generated by (A25).
- β_{xy} relates to the Chern number: $\tilde{G} = 2\beta_{xy} + \alpha_{xy}$, generated by (A26).

The rule for the Chern number’s parity, Eq. (5), follows from the last constraint here.

to $\hat{n} = (1, 0, 0, \dots)$ and all the planes bounding the Brillouin zone ($k_i = 0$) to $(-1, 0, 0, \dots)$. The Hamiltonian is defined as

$$H_c^{2s}(\mathbf{k}) = \hat{n} \cdot \mathbf{\Gamma}, \quad (\text{A32})$$

where $\mathbf{\Gamma}$ is the $(2s+1)$ -vector of gamma matrices. (A25) is an example of this construction for $d = 2s = 2$. The inversion matrix is given by the first gamma matrix: $I_0 = \Gamma^1$, and we can see that there are 2^{s-1} odd-parity occupied states at $\mathbf{k} = (\pi, \dots, \pi)$. At the other TRIMs, the occupied states have even inversion-parity.

The s^{th} Chern number C_s may be computed by the formula:

$$C_s = \frac{1}{s!} \left(\frac{i}{2\pi} \right)^s \int \text{Tr}[P(dP)^{2s}], \quad (\text{A33})$$

where $P(\mathbf{k}) = \frac{1}{2}(1 - H(\mathbf{k}))$ is the projector onto the filled states and d is the exterior derivative in the Brillouin zone. Evaluating the integral shows that $C_s = \pm 1$ for the Hamiltonian H_c^{2s} .

In $2s$ dimensions, Eq. (A23), generalized to more dimensions, gives a preliminary way of choosing the generators: H_β^{2s} is the image under j of a generator of $\pi_0(\tilde{\mathcal{H}}_{2s})$ and H_α^{2s} is an arbitrary preimage under ∂^{-1} of the generator of $\pi_0(\tilde{\mathcal{I}})_{2s-1}$. Any Hamiltonian can be expanded as

$$H = \beta_{2s} H_\beta^{2s} \oplus \alpha_{2s} H_\alpha^{2s}. \quad (\text{A34})$$

H_c^{2s} can be used for the generator H_α^{2s} . To see this, we decompose H_c^{2s} in terms of the original pair of generators $H_\alpha^{2s}, H_\beta^{2s}$. The s^{th} Chern number of H_β^{2s} is 2, since it is constructed using the map j which takes a general insulator to an inversion-symmetric one by duplicating it in each half of the Brillouin zone [see Eq. (A20)]. At all the TRIMs, $H_\beta^{2s}(\boldsymbol{\kappa}) = v_0$ and so n_o is zero. Using Eq. (A34) for H_c^{2s} implies

$$C_s(H_c^{2s}) = 1 = 2\beta_{2s} + \alpha_{2s} C_s(H_\alpha^{2s}), \quad (\text{A35a})$$

$$n_o(H_c^{2s}) = 2^{s-1} = 0 + \alpha_{2s} n_o(H_\alpha^{2s}). \quad (\text{A35b})$$

The first expression requires α_{2s} to be odd, and the second requires it to be a factor of 2^{s-1} . Hence $\alpha_{2s} = \pm 1$ and we can use H_c^{2s} as the generator H_α^{2s} . Since every Hamiltonian can be expressed by Eq. (A34), the number of odd inversion-parity states $n_o(\pi, \pi, \dots)$ is always a multiple of 2^{s-1} .

In terms of the general Hamiltonians in \mathcal{I}_{2s} , the total number of odd parity states at all the TRIMs must be a multiple of 2^{s-1} . Furthermore,

$$\frac{1}{2^{s-1}} \sum_{\text{TRIM } \mathbf{k}} n_o(\mathbf{k}) \equiv C_s \pmod{2} \quad \text{in } 2s\text{-dimensions.} \quad (\text{A36})$$

In $2s+1$ -dimensions, the Hamiltonians at $k_x = 0$ and π are both $2s$ -dimensional inversion-symmetric Hamiltonians, and they must have the same Chern number, so the

constraint on the parities is

$$\sum_{\text{TRIM } \boldsymbol{\kappa}} n_o(\boldsymbol{\kappa}) \equiv 0 \pmod{2^s} \quad \text{in } (2s+1)\text{-dimensions.} \quad (\text{A37})$$

This is related to the $(2s+1)$ -dimensional Chern-Simons integral $\theta_{2s+1} \in [0, 2\pi)$ by

$$\frac{\theta_{2s+1}}{\pi} = \frac{1}{2^s} \sum_{\text{TRIM } \boldsymbol{\kappa}} n_o(\boldsymbol{\kappa}) \pmod{2}, \quad (\text{A38})$$

because we can evaluate θ by writing the Hamiltonian as the $k_x = \pi$ cross-section of a Hamiltonian in one more dimension, and then determining the Chern number of that Hamiltonian⁶. The parity is given by (A37).

Appendix B: Tight Binding Models and Inversion Parity.

A useful example to study is a tight-binding model with one atom per unit cell which has some orbitals that are even, $|s_i\rangle$, where i ranges from 1 to N_{even} and some odd ones, $|p_i\rangle$, where i continues from $N_{\text{even}}+1$ to $N_{\text{odd}}+N_{\text{even}}$. Let the Hamiltonian be

$$H = - \sum_{i,j,\mathbf{R},\boldsymbol{\Delta}} t_{ij}(\boldsymbol{\Delta}) c_i^\dagger(\mathbf{R} + \boldsymbol{\Delta}) c_j(\mathbf{R}), \quad (\text{B1})$$

where c_i includes creation operators for both types of orbitals.

A Bloch wave function $\psi_{a\mathbf{k}}$ (a is the band index) is determined by its values at the origin, $\phi_i = \langle s_i/p_i | \psi_{a\mathbf{k}} \rangle$, for short) which are repeated in a plane-wave fashion to other sites. Inversion maps $\mathbf{k} \rightarrow -\mathbf{k}$ and $\phi_i \rightarrow I_{0ij} \phi_j$, where I_{0ij} is a diagonal matrix of N_{even} ones and N_{odd} minus ones.

There is a simple criterion for determining the parities of the occupied states at the TRIMs: if a state is odd, then all its s -wave components vanish. If it is even, all p -wave components vanish. In the generic case, it is enough to check a single s -wave component:

$$\begin{aligned} \eta_a(\boldsymbol{\kappa}) &= +1 \text{ if } \langle s_1 | \psi_{a\boldsymbol{\kappa}} \rangle \neq 0 \\ \eta_a(\boldsymbol{\kappa}) &= -1 \text{ (probably) if } \langle s_1 | \psi_{a\boldsymbol{\kappa}} \rangle = 0. \end{aligned} \quad (\text{B2})$$

If a component is exactly zero, it is reasonable to assume that it is because inversion symmetry forbids that component.

The Hamiltonian used to illustrate the entanglement-rule in Fig. 2 is of this type. In momentum space Eq. (B1) can be written $\sum_{ij} c_i^\dagger(\mathbf{k}) c_j(\mathbf{k}) H_{ij}(\mathbf{k})$. The Hamiltonian can be built from two subsystems H_1, H_2 , whose occupied states are given by the upper and lower signs in Fig. 2. Each Hamiltonian can be gapped because both sets of signs satisfy the constraint $\prod_{\boldsymbol{\kappa}} \eta_{\boldsymbol{\kappa}}$ by itself.

Each Hamiltonian H_r can be constructed in a space with one even state $|s_r\rangle$ and one odd state $|p_r\rangle$. For the

Hamiltonian to be inversion symmetric it must commute with σ_z , so the diagonal matrix elements are even and the off-diagonal matrix elements are odd functions of \mathbf{k} .

The two Hamiltonians can be combined together by including a small mixing between the two systems. The final Hamiltonian has the form:

$$H(\mathbf{k}) = \begin{pmatrix} H_1(\mathbf{k}) & t\mathbb{1} \\ t\mathbb{1} & H_2(\mathbf{k}) \end{pmatrix}. \quad (\text{B3})$$

where

$$\begin{aligned} H_1 &= A_{\mathbf{k}}\sigma_z + B_{\mathbf{k}}\sigma_x + C_{\mathbf{k}}\sigma_y \\ H_2 &= D_{\mathbf{k}}\sigma_z + E_{\mathbf{k}}\sigma_x + F_{\mathbf{k}}\sigma_y \end{aligned} \quad (\text{B4})$$

and

$$\begin{aligned} A_{\mathbf{k}} &= (1 - \cos(k_x)) \cos(k_y) + (1 + \cos(k_x)) \cos(k_y - k_z) \\ B_{\mathbf{k}} &= (1 - \cos(k_x)) \sin(k_y) + (1 + \cos(k_x)) \sin(k_y - k_z) \\ C_{\mathbf{k}} &= \sin(k_x), E_{\mathbf{k}} = -\sin(k_x), F_{\mathbf{k}} = \sin(k_z) \\ D_{\mathbf{k}} &= \cos(k_x) + \cos(k_z) - 1. \end{aligned}$$

The parities of the occupied states at κ of H_1 and H_2 under inversion in the point $\frac{1}{2}\hat{x}$ are equal to the signs shown in Fig. 2. Choosing this point to define the inversion parities is necessary because the entanglement spectrum is obtained by cutting the system between two planes of the atoms.

Appendix C: Monopoles

Consider a Hamiltonian for which the a^{th} and $a+1^{\text{st}}$ bands are close to being degenerate at \mathbf{k}_0 . Then all states except the two nearly degenerate states are unimportant, and the spectrum can be described by a 2×2 matrix

$$\mathcal{H}(\mathbf{k}) = \begin{pmatrix} E_0 + A(\mathbf{k}) & B(\mathbf{k}) \\ B^*(\mathbf{k}) & E_0 + C(\mathbf{k}) \end{pmatrix}. \quad (\text{C1})$$

The eigenvalues are degenerate wherever $A(\mathbf{k}) = C(\mathbf{k})$ and $B(\mathbf{k}) = 0$. This gives three equations in three variables (since B is complex), so generically, a solution may be found in three dimensional space, as pointed out by Von Neumann and Wigner.

Now at the location of the degeneracy (which we call \mathbf{k}_d) there is a magnetic monopole in the Berry magnetic fields \mathbf{B}_a and \mathbf{B}_{a+1} of the two bands. The degeneracy point (or Dirac point) has a handedness $\delta = \pm 1$, which determines the charge of the monopoles. Bands a and $a+1$ have opposite monopoles, of charge

$$\begin{aligned} Q_a &= 2\pi\delta \\ Q_{a+1} &= -2\pi\delta. \end{aligned} \quad (\text{C2})$$

This monopole and antimonopole are glued together (at the point \mathbf{k}_d) but they do not annihilate because they are monopoles in different magnetic fields.

To understand why the monopoles exist, write the Hamiltonian in terms of Pauli matrices, then expand the coefficients to linear order in \mathbf{k} , $H(\mathbf{k}) \approx E_0 + \mathbf{v}_0 \cdot \mathbf{k} + \sum_{i=1}^3 (\mathbf{v}_i \cdot \mathbf{k} \sigma_i)$. The handedness is defined by

$$\delta = \text{sign}[\mathbf{v}_1 \cdot (\mathbf{v}_2 \times \mathbf{v}_3)]. \quad (\text{C3})$$

Define the oblique coordinate system $K_i = (\mathbf{k} - \mathbf{k}_d) \cdot \mathbf{v}_i$. Now change to spherical coordinates, $K_3 = K \cos \theta$, $K_1 = K \sin \theta \cos \phi$, $K_2 = K \sin \theta \sin \phi$. The eigenvalues are $E_0 + \mathbf{v}_0 \cdot \mathbf{k} \pm K$. Note that if $\mathbf{v}_0 = 0$, then the graph of the energy as a function of K_1, K_2 with K_3 set to 0 is a cone. In accordance with the degrees-of-freedom-argument given above, fixing K_3 at a random value (and thus reducing the number of parameters to 2) gives a hyperboloid, without any touching between the bands.

The Berry magnetic field in band a is defined as $\mathbf{B}_a = \text{curl} \mathbf{A}_a$ where \mathbf{A}_a is defined in Eq. (15); note that the distinction between u and ψ does not matter for the purpose of calculating the magnetic field. The eigenvectors are $\psi_{a+1} = \begin{pmatrix} \cos \frac{1}{2}\theta e^{-i\phi} \\ \sin \frac{1}{2}\theta \end{pmatrix}$ and $\psi_a = \begin{pmatrix} \sin \frac{1}{2}\theta e^{-i\phi} \\ -\cos \frac{1}{2}\theta \end{pmatrix}$. The Berry connections for these states are $A_{a+1}(\mathbf{K}) = \frac{1}{2} \cot \frac{\theta}{2} \hat{\phi}$ and $A_a(\mathbf{K}) = \frac{1}{2} \tan \frac{\theta}{2} \hat{\phi}$. These fields are familiar as the vector potentials for Dirac monopoles²³—they have a flux-tube, or Dirac string, approaching the origin along the positive and negative K_3 axis. These monopoles have fluxes of $\oint \mathbf{B}_{a+1} = -2\pi$ and $\oint \mathbf{B}_a = 2\pi$ respectively.

The calculation just completed is incorrect half the time—the magnetic flux can be calculated in any coordinate system provided it is right-handed; it is a pseudoscalar. Hence, the result just obtained is correct when $\delta = +1$. When $\delta = -1$, the oblique coordinate system is left-handed, so the signs of the monopoles should be flipped, leading to Eq. (C2).

Now let us show that the curves defined by $s_a(\mathbf{k}) = 0$ and $s_{a+1}(\mathbf{k}) = 0$. (This appears in Sec. IIIB.) The function $s_a(\mathbf{k})$ is defined as $\langle s | \psi_{a\mathbf{k}} \rangle = \langle s | \uparrow \rangle \langle \uparrow | \psi_{a\mathbf{k}} \rangle + \langle s | \downarrow \rangle \langle \downarrow | \psi_{a\mathbf{k}} \rangle$ (since only the two states $|\uparrow\rangle$ and $|\downarrow\rangle$ that are represented by $\begin{pmatrix} 1 \\ 0 \end{pmatrix}$ and $\begin{pmatrix} 0 \\ 1 \end{pmatrix}$ in the effective theory are important near \mathbf{k}_d). So suppose

$$\begin{pmatrix} \langle \uparrow | s \rangle \\ \langle \downarrow | s \rangle \end{pmatrix} \propto \begin{pmatrix} \cos \frac{\alpha}{2} e^{-i\beta} \\ \sin \frac{\alpha}{2} \end{pmatrix}.$$

We then find that $s^a(\mathbf{k}) = 0$ only if $\theta = \alpha$ and $\phi = \beta$, and that $s^{a+1}(\mathbf{k}) = 0$ if $\theta = \pi - \alpha$ and $\phi = \pi + \beta$. That is, the two curves are rays meeting at the Dirac point from opposite directions.

Now let us see why a system cannot remain insulating when \mathbf{n}_o changes. When an even and odd state at a TRIM interchange, a pair of monopoles forms or annihilates. This may be seen using an effective Hamiltonian near the TRIM (say it is $\kappa = 0$). Eq. (C1) can be recycled for this problem. Since $I_0 H(\mathbf{k}) I_0^{-1} = H(-\mathbf{k})$, and $I_0 = \sigma_z$, the diagonal entries have to be even and the off-diagonal entries have to be odd functions of \mathbf{k} . Assume E_0 and the trace are equal to zero. (The trace just shifts

both bands by a smooth function and does not affect the degeneracy.) We wish to study how the dispersions change when $A(0) - C(0) = \Delta$, the difference between the two energies at the TRIMs, changes sign.

Let $A(\mathbf{k}) = \frac{\Delta}{2} + f(\mathbf{k}) = -C(\mathbf{k})$; f is a quadratic function to lowest order. $B(\mathbf{k})$ is a linear function of \mathbf{k} , so we may choose a coordinate system where the real and imaginary parts are K_1 and K_2 , $B(\mathbf{k}) = K_1 - iK_2$. The dispersion is therefore $\pm\sqrt{(\frac{\Delta}{2} + f(\mathbf{k}))^2 + K_1^2 + K_2^2}$. The states are degenerate if $\mathbf{K} = \mathbf{K}_d$ where $K_{d1} = K_{d2} = 0$ and $\Delta = -2f(K_{d3}, 0, 0) = -2\alpha K_{d3}^2$, say. Thus, if $\alpha > 0$, there are band-touchings when Δ is negative (with $K_{d3} = \pm\sqrt{-\frac{\Delta}{2\alpha}}$) and no crossings when Δ is positive. So if Δ changes from positive to negative, two monopoles appear. The crossings move out from the origin to a distance proportional to the square root of Δ .

Now reexpand the Hamiltonian to linear order around \mathbf{K}_d . We find that it is equal to $\alpha K_{d3}(K_3 - K_{d3})\sigma_z + K_1\sigma_x + K_2\sigma_y$. (Notice that we have set $K_1 = K_2 = 0$ in $f(K_1, K_2, K_3)$ because we are interested in values of the K 's such that $K_1, K_2 \ll K_3$. The orders of magnitude such that all the terms under the square root in the dispersion have the same magnitude are $K_1 \sim \Delta$, $K_2 \sim \Delta$, $K_3 \sim \sqrt{\Delta}$.) The two cone points have opposite handedness since K_{d3} has opposite signs. This was what we expected since the monopole charge has to be conserved.

Appendix D: Entanglement Spectrum

The flat band Hamiltonian is defined in terms of the correlation function $C(x_1, x_2) = \langle \psi(x_2)^\dagger \psi(x_1) \rangle$. (Once the results are derived in one dimension, the three dimensional results can be written out by including factors of $e^{i\mathbf{k}_\perp \cdot \mathbf{r}}$.)

Because the correlation function decays exponentially (for an insulator), it is reasonable to think of it as a hopping matrix for an electron system:

$$[H_{\text{flat}}\phi](x) = \frac{1}{2}\phi(x) - \int C(x, x')\phi(x')dx'. \quad (\text{D1})$$

The eigenfunctions of this Hamiltonian are the same as the eigenfunctions of the physical system but the eigenvalues are different. Each unoccupied state ϕ_γ has eigenvalue $\frac{1}{2}$ and each occupied state belongs to an eigenvalue $-\frac{1}{2}$, since $C(x_1, x_2) = \sum_\gamma \phi_\gamma(x_1)\phi_\gamma(x_2)^*$.

When a surface at $x = 0$ is introduced we can split the wave function into two parts, $x > 0$ and $x < 0$, and represent them as the top and bottom halves of state-vectors. Then the correlation function has four parts,

$$\hat{C} = \begin{pmatrix} \hat{C}_L & \hat{C}_{RL}^\dagger \\ \hat{C}_{RL} & \hat{C}_R \end{pmatrix}. \quad (\text{D2})$$

The entanglement eigenstates f_i^L turn out²⁰ to be the eigenfunctions of $H_L = \frac{1}{2}\mathbf{1} - \hat{C}_L$.

The eigenvalues are called $\frac{1}{2} - p_i(\mathbf{k}_\perp)$. These eigenvalues are between $\pm\frac{1}{2}$ because p_i is the probability that an electron occupies the state f_i^L . Any eigenvalue in the range $0 < p_i < 1$ is a state in the gap, so the wavefunction is localized near the surface. There are *infinitely* many surface states like this. In three dimensions, if they are graphed as functions of \mathbf{k}_\perp , the highest bands converge to $\pm\frac{1}{2}$.

The entanglement energy spectrum is not quite the same as p_i but is related by the transformation $\epsilon = 2\tanh^{-1}(1 - 2p)$ which sends the limiting energies to $\pm\infty$; $p = \frac{1}{2}$ corresponds to $\epsilon = 0$. The graphs of the entanglement energies look more normal—they retain a finite spacing, although there are infinitely many of them.

Since \hat{C} has 1 and 0 as eigenvalues, $\hat{C}^2 = \hat{C}$, giving four matrix equations. For showing how to pair eigenstates²¹ of \hat{C}_L and \hat{C}_R , the relevant equation is $\hat{C}_{RL}(\mathbf{1} - \hat{C}_L) = \hat{C}_R\hat{C}_{RL}$. Given an eigenfunction f_i^L of \hat{C}_L with eigenvalue p_{Li} one can obtain an eigenvector of \hat{C}_R with eigenvalue $1 - p_i$ via the transformation \hat{M}

$$f_i^R(x) = [\hat{M}f_i^L](x) = \frac{1}{\sqrt{p_i(1-p_i)}} \sum_{x'>0} \hat{C}_{RL}(x, x')f_i^R(x'). \quad (\text{D3})$$

The prefactor is inserted to ensure that f_i^R is normalized. Because of how p transforms, $\epsilon_{Li} = -\epsilon_{Ri}$. (One can check that \hat{M} is a unitary transformation, which can be written in matrix form $\hat{M} = \frac{1}{\sqrt{\hat{C}_R - \hat{C}_R^2}}\hat{C}_{RL}$.) The eigenvalues of f_i^L and f_i^R for H_L and H_R are $\pm(\frac{1}{2} - p_i)$ and $\epsilon_{Li} = -\epsilon_{Ri}$.

Furthermore, $F_i = \sqrt{p_i}f_i^L + \sqrt{1-p_i}f_i^R$ is an occupied state because it satisfies $\hat{C}|F_i\rangle = |F_i\rangle$. (Eq. (24) restates this obscurely.) States of this form give a basis for all the occupied states. The ground state is therefore given by $\prod_i (\sqrt{p_i}l_i^\dagger + \sqrt{1-p_i}r_i^\dagger)|vac\rangle$ where l_i^\dagger, r_i^\dagger create the states f_i^L and f_i^R respectively. Cross-multiplying gives the Schmidt decomposition, Eq. (22). The state F_i is definitely occupied by an electron. This electron is on the left with probability p_i and on the right with probability $1 - p_i$. A term in the Schmidt decomposition is obtained by making a choice, for each mode, whether the electron is on the left or right.

If a state is filled on the left side, then the corresponding state must be left empty on the right. Thus the Schmidt states are $|\alpha\rangle_L = \prod_{i \in A} l_i^\dagger |vac\rangle_L$ and $|\alpha\rangle_R = \prod_{i \notin A} r_i^\dagger |vac\rangle_R$ where A is a set of states. The weight of this state is $\prod_{i \in A} p_i \prod_{i \notin A} (1 - p_i)$.

To reinterpret the fluctuations as statistical fluctuations of the system on the left, imagine covering the right half. Then electrons disappear when they cross the boundary. The factors of r_i^\dagger correspond to holes in $|\alpha\rangle_L$. The weight of a state can be written in terms of just the occupied states on the left by factoring out $\frac{1}{2} := \prod_i (1 - p_i)$. The weight is then $\prod_{i \in A} \frac{p_i}{1 - p_i}$ which looks like a Boltzmann distribution if $e^{-\epsilon_{Li}} := \frac{p_i}{1 - p_i}$, explaining where the definition of ϵ_{Li} comes from.

The maximum weight Schmidt state is obtained by

placing electrons on the left half when $p_i > \frac{1}{2}$ and on the right half when $p_i < \frac{1}{2}$. If we can only see the left half, this is equivalent to filling all the negative “energy” states. The negative energy states on the right are also filled since $\epsilon_{Ri} = -\epsilon_{Li}$. So the maximum weight state is the product $|G\rangle_L|G\rangle_R$ of the ground states of H_L and H_R .

Appendix E: Parity of Arcs through a TRIM

Suppose $\Delta N_e(\mathbf{\kappa}_\perp)$ is prescribed at a certain TRIM. The number of arcs passing through this TRIM must be equal to $\Delta\nu$ modulo 2. To show this, we use the $k \cdot p$ effective Hamiltonian in the space of states that have energy zero at $\mathbf{\kappa}_\perp$ to determine how the energies vary away from $\mathbf{\kappa}_\perp$. Suppose for simplicity that all the modes at the TRIM have the same \mathcal{I}_e parity (the generic case). Then particle-hole symmetry implies that the effective Hamiltonian is odd in \mathbf{k}_\perp , to leading order $H(\mathbf{k}_\perp) = A_x k_x + A_y k_y + \dots$. Hence $H(\mathbf{k}_\perp) = |k|(A_x \cos \theta + A_y \sin \theta)$, in polar coordinates. The energy-dependence has a cone-like structure: $\epsilon_i(k, \theta) = |k|f_i(\theta)$ where $f_i(\theta)$ are the eigenvalues of the periodic Hamiltonian $A_x \cos \theta + A_y \sin \theta$. Now the particle-hole symmetry implies that the bands come in pairs satisfying $\epsilon_i(\mathbf{k}_\perp) = -\epsilon_{i'}(-\mathbf{k}_\perp)$, or in other words that $f_i(\theta + \pi) = -f_{\Delta N_e + 1 - i}(\theta)$. Thus between θ and $\theta + \pi$, the energies must be turned upside down. This relates the dispersions f_i in pairs, except for the middle one $f_{\frac{1}{2}(\Delta N_e + 1)}$ (if ΔN_e is odd) which is related to itself. This mode changes sign from 0 to π by the symmetry, so it crosses through 0 at an odd number $2k+1$ of values of θ in between, and crosses zero again at $2k+1$ points 180° away. When the solutions to $\epsilon_i(\mathbf{k}_\perp) = 0$ are graphed, these crossings correspond to $2k+1$ arcs passing through the TRIM. The other pairs of modes f_i and f_{N+1-i} together give rise to an even number of arcs. Thus, the parity of the number of Fermi arcs is equal to the parity of ΔN_e .

Though the parity of the number of arcs is determined by ΔN_e 's parity, the precise number of arcs is not. For example, when $\Delta N_e = 2$, there may be no zero-energy states away from the TRIM, as in the Dirac equation.

Appendix F: Polarization

From the point of view of standard electrostatics, one expects a cubic crystal, aligned with the x, y , and z axes, with polarization \mathbf{P} , to have a surface charge of P^x per unit cell on the yz surfaces. However, in general, a material may have some stray charges on the surface.

In some situations, the surface charge is expected to be determined (almost) by the theoretical value of the polarization¹⁶. This does not always happen because there may be extra charge trapped on the surface. But for a *clean* surface (that is, a perfectly periodic one) the ambiguity can be reduced: the charge density per unit

cell is given by P^x up to an integer multiple of e , if the surface is gapped.

If there are no modes at the Fermi energy on the surface, then $P^x = Q_x + ke$ (the surface charge per unit cell). The surface charge may be changed by ke by filling k surface bands. It is not possible to add a fractional multiple of e to each cell, since then the surface will become conducting, according to the theorem that an insulator must have a whole number of electrons per unit cell, unless strong interactions produce an unusual phase. (Since we are assuming time reversal to be broken, generically, an odd number of electrons *can* form an insulator.)

This prediction for the surface charge may be generalized to allow for a metallic surface. In this case there is a two dimensional Fermi surface describing the modes on the surface. The polarization is

$$P^x \equiv Q_x - \frac{eA_{fs}}{(2\pi)^2} \pmod{e}. \quad (\text{F1})$$

where A_{fs} is the area of the surface arcs. The second term can be interpreted as the charge that needs to be removed to make the surface insulating.

If a crystal has a fractional polarization of P^x , then there are three possibilities. The surface may be electrically charged (with a density of $P^x + ke$ per unit cell for some integer k), or it may be metallic. The surface may also reconstruct, so that there is a charge density wave. When P^x is a simple fraction, this is very likely, since then the charge density wave would be commensurate. For example, when $P^x = \frac{e}{2}$ (as expected for inversion-symmetric insulators) the surface could have a period two reconstruction. The surface might also be metallic, but a big spontaneous surface charge seems unlikely. Since the “intrinsic” polarization may be exchanged for a surface property, a scanning tunneling microscope may be the best tool for observing it.

The polarization may be determined by noting that the entanglement Hamiltonian H_L has to satisfy the same constraints on its surface charge. We can just determine Q_x and A_{fs} for the ground state of H_L . Assume $\mathbf{G}_H = 0$. Then the number of arcs through each TRIM has the same parity, either even or odd (according to Eq. (7)). The Fermi surface covers half the Brillouin zone if this number is odd, so according to Eq. (23),

$$\begin{aligned} \frac{A_{fs}}{(2\pi)^2} &\equiv \frac{1}{4}(\Delta N(0, 0, 0) + \Delta N(\pi, 0, 0)) \\ &\equiv \frac{n}{2} - \tilde{P}_e^x \pmod{1} \end{aligned} \quad (\text{F2})$$

where \tilde{P}_e^x is defined by Eq. (18). The second line uses $\Delta N(\mathbf{\kappa}) = n - 2n_o(\mathbf{\kappa})$

Now, if there are no nuclei at $x = 0$, then as in Sec. IV, one can use the neutrality of the Schmidt spectrum and symmetry to show that $Q_x = 0$. If on $x = 0$ there are nuclei of total atomic number per cell Z_0 , imagine taking these nuclei out of the system. This leaves behind a charge of $Z_0 e$ which must be divided evenly between the

left and right half. Focus on the left half of the system; it has a charge of $Q_x = \frac{Z_0 e}{2}$.

Now substitute Q_x and A_{fs} into Eq. (F1). Combine the n term in Eq. (F2) with Q_x to get $\frac{(Z_0 - n)e}{2}$. By neutrality n is the total atomic number per unit cell, so $n - Z_0$ is the atomic number of the nuclei not on $x = 0$, which is congruent mod 2 to $Z_{\frac{1}{2}}$ (the number of nuclei at $x = \frac{1}{2}$) because the other nuclei come in pairs. Hence the polarization is $e\tilde{P}_e^x - \frac{1}{2}Z_{\frac{1}{2}}e$. This agrees with Eq. (8) because the dipole moment of the nuclei relative to $x = 0$ is $-\frac{1}{2}Z_{\frac{1}{2}}e$. Nuclei not on the two special planes 0 and $\frac{1}{2}$ come in pairs and cancel out. (We are defining the dipole moment of the nuclei to be the sum over a unit cell bounded by $-\frac{1}{2} < x \leq \frac{1}{2}$ in the x -direction.)

Appendix G: Frozen Crystals

This appendix determines what subset of the space of \mathbf{n}_o vectors is spanned by integer combinations of frozen crystals. Let \mathbf{f}_p be vectors corresponding to systems with a single fixed electron in each unit cell displace by \mathbf{p} from the Bravais lattice.

For each of the 7 nonzero polarizations \mathbf{p} , \mathbf{f}_p is represented by a vector with four ones and four zeros ($\mathbf{f}_p(\boldsymbol{\kappa}) \equiv \frac{\boldsymbol{\kappa}}{\pi} \cdot \mathbf{p} \pmod{2}$). This assumes the electron to be in an even orbital. For $\mathbf{p} = 0$, take the electron to be in an odd orbital instead so that $\mathbf{f}_0(\boldsymbol{\kappa}) = 1$.

The goal is now to determine what vectors are integer linear combinations of the \mathbf{f} 's. There is a coordinate system for \mathbb{Z}^8 where this is easy to solve. One has to find a set of vectors $\mathbf{v}_1 \dots \mathbf{v}_8$ such that it is a basis for \mathbb{Z}^8 , and also $n_1 \mathbf{v}_1, n_2 \mathbf{v}_2, \dots, n_8 \mathbf{v}_8$ is a basis for the frozen vectors (where n_1, \dots, n_8 are certain integers). Then if a vector \mathbf{n}_o is represented by $a_1 \mathbf{v}_1 + \dots + a_8 \mathbf{v}_8$ in the new coordinate system, the criteria that it is a frozen vector are simple— a_i has to be a multiple of n_i . The classification theorem for finitely generated abelian groups describes an algorithm for finding such bases.

To find the basis, take an 8×8 matrix whose columns are the \mathbf{f} 's and do column operations. The only opera-

tions that are allowed are adding or subtracting multiples of one column to another or changing the sign of a column. These operations do not change the lattice spanned by the \mathbf{f} 's. (They can be inverted without dividing by integers.)

This process leads to the following basis: $\mathbf{v}_0, \mathbf{v}_x, 2\mathbf{v}_{xy}$, and $4\mathbf{v}_{xyz}$ and vectors symmetric with these. Here, \mathbf{v}_0 is the vector with ones at all corners of the cube, \mathbf{v}_x is the vector with ones on the *face* of the cube defined by $\kappa_x = \pi$ (and zeros elsewhere), \mathbf{v}_{xy} is the vector with ones on the *edge* defined by $\kappa_x = \kappa_y = \pi$, and \mathbf{v}_{xyz} is the vector with a one at the *vertex* $\kappa_x = \kappa_y = \pi$.

The procedure for changing the basis from $\mathbf{f}_0, \mathbf{f}_i, \mathbf{f}_{ij}, \mathbf{f}_{xyz}$ to $\mathbf{v}_0, \mathbf{v}_i, 2\mathbf{v}_{ij}, 4\mathbf{v}_{xyz}$ (where i, j run over x, y, z) consists of changing one of the four groups of \mathbf{f} 's to \mathbf{v} 's at a time. First $\mathbf{f}_0 = \mathbf{v}_0, \mathbf{f}_i = \mathbf{v}_i$ so we can just rename the sequence of vectors $\mathbf{v}_0, \mathbf{v}_i, \mathbf{f}_{ij}, \mathbf{f}_{xyz}$. Next, replace $\mathbf{f}_{\frac{1}{2}(\hat{x}+\hat{y})}$ by $-(\mathbf{f}_{\frac{1}{2}(\hat{x}+\hat{y})} - \mathbf{v}_x - \mathbf{v}_y)$, which is equal to $2\mathbf{v}_{xy}$. This is one of the column operations just described (it changes a vector in the third set by adding other vectors to it). Do the same for the other pairs of x, y, z . Last replace $\mathbf{f}_{\frac{1}{2}(\hat{x}+\hat{y}+\hat{z})}$ by

$$4\mathbf{v}_{xyz} = \mathbf{f}_{\frac{1}{2}(\hat{x}+\hat{y}+\hat{z})} - \mathbf{v}_x - \mathbf{v}_y - \mathbf{v}_z + 2\mathbf{v}_{xy} + 2\mathbf{v}_{yz} + 2\mathbf{v}_{xz}.$$

Each of these relations makes the ones cancel out except on just the right vertex or edge of the cube.

Some thought leads to a similar demonstration that $\mathbf{v}_0, \mathbf{v}_i, \mathbf{v}_{ij}$ and \mathbf{v}_{xyz} (without the factors of 2 and 4) span *all* combinations of 8 integers. Therefore any vector \mathbf{n}_o can be decomposed as

$$\mathbf{f} = a_0 \mathbf{v}_0 + \sum_i a_i \mathbf{v}_i + \sum_{i < j} a_{ij} \mathbf{v}_{ij} + a_{xyz} \mathbf{v}_{xyz} \quad (\text{G1})$$

where a_{ij} is an even integer and a_{xyz} is a multiple of four. An even part of a_{ij} and a multiple of 4 contained in a_{xyz} can be combined with the a_0, a_i -terms to form a vector that represents an inert insulator \mathbf{f} , leaving the remainder given in Eq. (21).

The concise statement of this result is that the quotient of \mathbb{Z}^8 by the span of the \mathbf{f} 's is $\mathbb{Z}_2^3 \times \mathbb{Z}_4$.

¹ Hasan, M.Z. and C. L. Kane, arXiv:1002.3895; Qi, X.-L. and S.-C. Zhang, arXiv:1008.2026; Moore, J.E., Nature **464**, 194 (2010).

² A.P. Schnyder et al., Phys. Rev. B **78**, 195125;

³ Kitaev, A., in Proceedings of the L. D. Landau, Chernogolokova (Russia), Memorial Conference “Advances in Theoretical Physics,” **1134**, 22-30, AIP, Melville, NY (2009).

⁴ Mong, R., A. M. Essin, J. E. Moore, Physical Review B **81**, 245209 (2010).

⁵ Chen, Y.L. et al., Science, **329**, 659 - 662 (2010).

⁶ Qi, X.-L., T.L. Hughes and S.-C. Zhang, Phys. Rev. B **78**, 195424 (2008).

⁷ Essin, A.M., J.E. Moore., and Vanderbilt, D., Phys. Rev. Lett. **102**, 146805 (2009).

⁸ Fu, L. and C. L. Kane. Phys. Rev. B **76**, 045302 (2007).

⁹ Wang, Zhong, Xiao-Liang Qi and Shou-Cheng Zhang. New J. Phys. **12**, 065007 (2010).

¹⁰ Murakami, Shuichi New J. Phys. **9**, 356 (2007).

¹¹ Fidkowski, L. Phys. Rev. Lett. **104** (2010).

¹² Turner, Ari M., Yi Zhang, and Ashvin Vishwanath, arXiv:0909.3119.

¹³ Rodriguez, I. and G. Sierra, Phys. Rev. B **80** (2009); Bray-Ali, N., L. Ding and S. Haas, Phys. Rev. B **80** (2009); Haldane, F.D.M., APS 2009 March Meeting Proceedings (unpublished).

- ¹⁴ Wan, Xiangang, Ari Turner, Ashvin Vishwanath, and Sergey Y. Savrasov, arXiv:1007.0016.
- ¹⁵ Resta, R. and D. Vanderbilt in Topics in Applied Physics **105**, 31. Berlin: Springer-Verlag (2007).
- ¹⁶ Vanderbilt, David and R. D. King-Smith, Phys. Rev. B **48**, 442 (1993).
- ¹⁷ Thouless, D.J., M. Kohmoto, M. P. Nightingale, and M. DenNijs, Phys. Rev. Lett. **49**, 405 (1982).
- ¹⁸ Avron, J. E., R. Seiler, and B. Simon, Phys. Rev. Lett. **51**, 51 (1983).
- ¹⁹ Moore, J. E., Y. Ran and X. G. Wen. Phys. Rev. Lett. **101**, 186805 (2008).
- ²⁰ Peschel, I., J. Phys. A., **36**, L205 (2003).
- ²¹ Botero, A. and B. Reznik, Phys. Lett. A, **331**, 39 (2004); Klich, I., J. Phys. A **39**, L85 (2006).
- ²² Nakahara, M., Geometry, Topology and Physics (2nd ed.), Bristol: Institute of Physics Publishing (2003); Hatcher, Allen, Vector Bundles and K-Theory, www.math.cornell.edu/~hatcher/VBKT/VBpage.html; Hatcher, Allen, Algebraic Topology, Cambridge: Cambridge University Press (2002); “Geometry, Topology and Physics” presents algebraic topology with some applications to physics, and in particular works out the homotopy groups of $U(n)$ using Chern numbers. The topic of “Vector Bundles and K-Theory” is closely related to classifying topological insulators. (The “K-group” of a d -dimensional torus is basically the set of classes of topological insulators in d -dimensions, under the operation of direct sum.) “Algebraic Topology” explains the exact sequence used in appendix A.
- ²³ Jackson, J.D., Classical Electrodynamics (3rd ed.), New York: Wiley (1999).
- ²⁴ This follows from the relation between topological insulators and the homotopy groups of Grassmann spaces $\mathcal{G}_{n,m}$; the essential fact is that the homotopy group $\pi_{2s}(\mathcal{G}_{s,N-s}) = \mathbb{Z}$ when N is sufficiently large²².
- ²⁵ There are technical problems when an orbital $|\alpha\rangle$ is at a half-lattice vector—choosing which copy of it belongs to the unit cell breaks inversion symmetry. The simplest solution is to slice the orbital into two parts that are images of each other under inversion, $|\alpha\rangle = \frac{1}{\sqrt{2}}(|\alpha_1\rangle \pm |\alpha_2\rangle)$. The opposite combination of these orbitals is then assigned a very large energy so that it has no effect.
- ²⁶ In a sequence such as $U(1), U(2)$, *etc.*, the homotopy groups of the first few elements are irregular, but eventually stabilizes farther in to the sequence.
- ²⁷ In one dimension, this construction gives a basis of localized occupied states, somewhat like Wannier orbitals. Each of the f^L and f^R states, which have energies in the gap, are confined to some layer near the surface. Their sum is an eigenstate of H_{flat} . (Unlike the Wannier basis, these states are all localized around the same bond.) The Hamiltonian H_{flat} has localized eigenfunctions, unlike most Hamiltonians, because the dispersion relation is flat, and so the group velocity is equal to zero.
- ²⁸ The Hamiltonian we are classifying ($H'(k) = H(k) \ominus H(0)$) is one of the generalized Hamiltonians defined above; that is why a number of bands n_e or n_o can be negative.